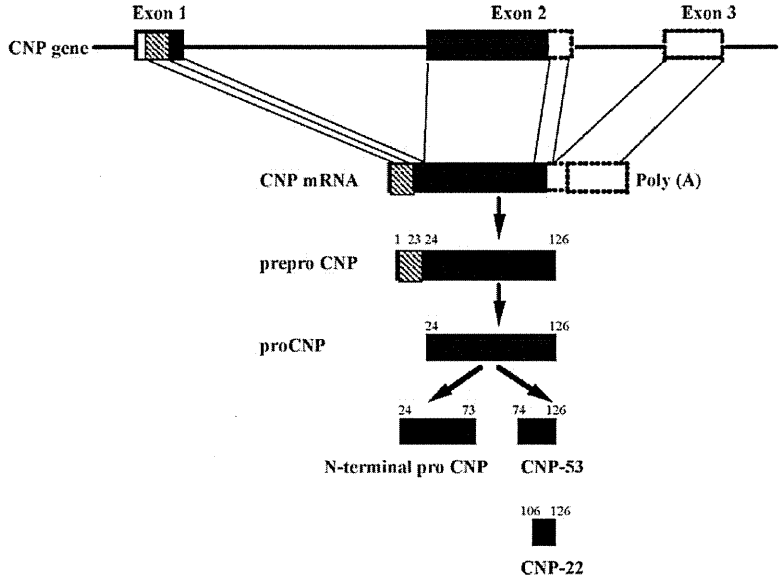

Figure 4 Structure of the gene and biosynthetic pathway of human CNP. mRNA: messenger RNA.

are essentially the same. Furin is thought to cleave proCNP into CNP-53 [14], whereas PC2 and/or PC1/3 are thought to cleave proCNP into CNP. CNP-53 is generally the major endogenous tissue molecular form [15].

Tissue distribution and gene expression

ANP

ANP is abundantly expressed in the heart, such that tissue levels of ANP are 250–1000-fold higher in atrium than in ventricle. The atrium is the major site of ANP synthesis, and ANP mRNA levels are considerably higher in the atria than in the ventricles. High levels of both ANP mRNA and ANP are found in the ventricles of neonatal rats, but these levels rapidly decline in parallel with the change in cardiac contractile protein isoforms that occurs after birth [4]. As a result, healthy adult ventricular tissue actually produces little ANP. However, ventricular ANP expression is re-induced in the hypertrophied and failing heart, making the ventricle a substantial source of circulating ANP in cases of severe heart failure [16].

ANP mRNA has also been detected in a variety of extracardiac tissues, including the hypothalamus, pituitary gland and lung [17], but the extracardiac expression is generally weak. Within the central nervous system, the highest ANP concentrations are in the hypothalamus and septum. The major molecular forms of ANP as a neuropeptide are α-ANP(4–18) and α-ANP(5–28) [18]. Thus, the molecular forms of the ANP neuropeptide differ from those of the ANP cardiac peptide. Finally, urodilatin, an N-terminal 4-amino acid-extended form of α-ANP derived from γ-ANP, was identified in urine. Its site of production is the kidney [19].

BNP

Concentrations of BNP and its mRNA are much lower in the human cardiac ventricle than in the atrium, but the total content of BNP and its mRNA in the ventricle accounts for 30% and 70% of that in the whole heart, respectively [20]. A clinical study also showed that plasma BNP levels are higher in the anterior interventricular vein and the coronary sinus than in the aortic root, suggesting BNP is a cardiac hormone that is predominantly synthesized in and secreted from the ventricle [21]. In addition, no appreciable amount of BNP has been detected in the rat or human brain, suggesting that the tissue distribution of BNP differs among species.

ProBNP-108 is most likely cleaved by a processing enzyme to BNP-32 and NT-proBNP-76 as it is secreted [10]. Levels of myocardial BNP mRNA and circulating BNP and NT-proBNP-76 are obviously increased as compared with those of ANP in patients with congestive heart failure, which suggests BNP functions as an emergency defense against ventricular overload in disease states.

One of the characteristic features of BNP mRNA that sets it apart from ANP mRNA is a conserved sequence consisting of repeated AUUUA units in the 3′ untranslated region (Fig. 3). The presence of this sequence accelerates the degradation of BNP mRNA in a manner similar to that seen with lymphokine genes and oncogenes [22]. Thus, BNP gene expression is regulated differently from ANP gene expression and is thought to dynamically change, depending on the physiological and pathophysiological conditions.

CNP

CNP is distributed throughout the brain in rats and humans, and a substantial amount is present in pituitary gland in rat. Consequently, CNP was initially thought to act as a neuropeptide [22]; however, subsequent studies showed that CNP is also synthesized in kidney, bone, blood cells, blood vessels and heart [23]. For example, cultured vascular endothelial cells (ECs) reportedly show significant CNP gene expression and peptide secretion [24]. CNP secretion from ECs is stimulated by such cytokines as transforming growth factor, tumor necrosis factor, interleukin-1, basic fibroblast growth factor, and lipopolysaccharide. This suggests CNP

may be active in the vascular wall under various pathological conditions [25]. On the other hand, initial studies failed to detect CNP mRNA in human or rat heart, and the low levels of CNP immunoreactivity detected in pig and human hearts were thought to reflect cross-reactivity with ANP or products from coronary arterial ECs [26]. Subsequent immunohistochemical and reverse transcription polymerase chain reaction analyses confirmed the presence of CNP and its mRNA in both the atrium and ventricle, and a recent *in vitro* study verified that a significant amount of CNP is expressed in and secreted from cultured rat cardiac fibroblasts, but not myocytes, indicating a cardiac expression profile that is distinctly different than those of ANP and BNP [27].

Molecular mechanism regulating natriuretic peptide gene expression

Transcriptional regulation of ANP gene expression

Studies using transgenic mice carrying a 500-bp segment of the 5′ flanking region (5′-FR) of the human ANP gene fused to a gene encoding SV40 large T antigen, a 2.4-kbp 5′-FR segment of human ANP gene fused to the chloramphenicol acetyltransferase gene, or a 638-bp or 3-kbp 5′-FR segment of the rat ANP gene fused to the luciferase gene have shown that the proximal 5′-FR of the ANP gene is sufficient to recapitulate the spatial and temporal expression of the endogenous ANP gene, and that the region contains sequences important for the regulation of ANP gene expression in the heart [28–30]. Indeed, expression of a reporter gene driven by the proximal 5′-FR of the ANP gene in atrial or ventricular cardiac myocytes at different developmental stages showed that the region confers proper spatial and temporal activity to the ANP promoter [31,32]. The proximal 5′-FR of the ANP gene contains multiple transcription factor-binding sites, including two CArG boxes, two NKEs, three TBEs, two GATA sites, an A/T-rich element and a phenylephrine-responsive element (PERE), to which the transcriptional factors SRF, NKX2.5, Tbx5, GATA4/6, MEF2C and Zfp260 have been shown to bind [33,34]. These transcriptional factor-binding elements contribute singly and cooperatively to the basal and inducible activation of ANP promoter activity in cardiac cells [33,34]. In addition, neuron-restrictive silencer element (NRSE), hypoxia-response element (HRE) and glucocorticoid responsive element (GRE), which are located outside the proximal promoter, also reportedly mediate inducible ANP gene transcription [33,36]. In that regard, differences in the expression pattern of the proximal 5′-FR of the ANP gene and the intact endogenous ANP gene highlight the importance of regulatory elements outside the proximal 5′-FR [33]. It also should be noted that the ANP gene is located 8 kbp and 12 kbp downstream of the BNP gene on the same chromosome in humans and mice, respectively (human, chromosome 1; mouse, chromosome 4) [37,38].

Transcriptional regulation of BNP gene expression

The 5′-FR of the BNP gene has also been studied so as to better understand the regulatory mechanisms governing the gene's cardiac-specific and inducible expression. A study using transgenic mice carrying a 5′-FR segment of the human BNP gene extending from −1818 to +100, or from −408 to +100, coupled to a luciferase gene (−1818hBNPluc and −400hBNPluc, respectively) showed that the proximal region of the human BNP promoter is sufficient to mediate ventricle-specific expression [39]. The luciferase activity of −1818hBNPluc was also greater in ventricular myocytes than in atrial myocytes [40]. In addition, deletion analysis showed that the region extending from −127 to −40 of the human BNP 5′-FR confers cardiac-specific expression [40]. This proximal region of the human BNP promoter contains potential GATA, M-CAT and AP-1/CRE-like elements, which are conserved among humans, rats and mice [41].

All three of the aforementioned elements are known to regulate cardiac-specific gene expression, and have been shown to mediate both basal and inducible BNP gene expression [41]. Other sites located in relatively distal regions of the human BNP 5′-FR, including NRSE (−552), shear stress-responsive elements [SSRE] (−652, −641 and 161), thyroid hormone-responsive element (TRE) (−1000) and the nuclear factor of activated T-cells (NF-AT) binding site (−927), have also been shown to participate in inducible activation of the human BNP promoter [41,42]. Among these elements, the transcriptional repressor element NRSE, which is located at −552 in the human BNP promoter and is conserved in the rat and mouse BNP promoters, represses basal BNP promoter activity and mediates hypertrophic signaling evoked with extracellular matrix [43]. A transcriptional repressor, neuron restrictive-silencer factor (NRSF, also named as REST), binds to NRSE, thereby repressing promoter activity. Interestingly, NRSE is also located in the 3′ untranslated region of the ANP gene and is involved in basal and endothelin-1-inducible activation of human ANP transcription [35]. Moreover, cardiac-restricted inactivation of NRSF through overexpression of a dominant-negative NRSF driven by the cardiac-specific a-MHC promoter leads to up-regulation of ventricular ANP and BNP gene expression, cardiomyopathy and sudden death, which confirms the importance of NRSF in the regulation of cardiac gene expression and cardiac function [36]. Although BNP gene expression is reportedly under the control of SRF, as is the case with ANP gene expression, a functional CArG box had not been identified in the proximal 5′-FR of the BNP gene [44]. However, we recently identified a conserved and functional CArG box in the BNP 5′-FR, and showed that Rho- and actin dynamics-dependent signaling activates BNP gene expression through this element by inducing translocation of a novel SRF co-factor, myocardin-related transcription factor (MRTF)-A (also named as MAL or MKL1) [45,46].

Transcriptional regulation of CNP gene expression

Transcriptional regulation of CNP has received much less attention than that of ANP and BNP. It is known, however, that two GC-rich elements in the CNP promoter play an important role in regulating CNP gene expression [47]. TSC22D1, a leucine zipper protein, and STK16 (TSF-1), a protein possessing both DNA-binding ability and serine-threonine kinase activity, have been identified as transcription factors that bind to the GC-rich element [48,49].

ANP and BNP as diagnostic markers of cardiovascular disease

Plasma levels of ANP and BNP are increased under such pathological conditions as heart failure, myocardial infarction, hypertension, left ventricular hypertrophy and pulmonary hypertension.

Heart failure

Initial studies demonstrated that plasma ANP levels increase in proportion to the severity of symptomatic congestive heart failure [50]. Similarly, levels of both ANP and BNP increase and their secretion profiles vary according to the underlying cardiac condition in patients with severe heart failure [51]. Several studies have also shown that plasma ANP levels are significantly elevated in asymptomatic patients with left ventricular dysfunction. Conversely, the severity of heart failure has been evaluated based on plasma BNP levels, which closely correlate with NYHA functional class and hemodynamics [21]. In addition, plasma ANP levels increase in response to increases in right and/or left atrial pressure, while increases in BNP reflect the degree of ventricular overload. Plasma BNP levels are also useful for identifying patients with asymptomatic left ventricular dysfunction, and several investigators have found that they can serve as diagnostic markers of left ventricular systolic dysfunction both in the general population and in patients with cardiovascular disease [52]. Furthermore, low BNP levels can be used to rule out congestive heart failure in symptomatic individuals with higher negative predictive values. In the urgent care setting, rapid measurement of BNP values is useful for establishing or excluding a diagnosis of congestive heart failure in patients with acute dyspnea [53]. Thus, measuring BNP levels is useful not only for evaluating the severity of heart failure, but also for excluding and screening for left ventricular dysfunction and heart failure. For these reasons, authoritative guidelines on the clinical diagnosis and management of heart failure recommend measuring BNP [54–56].

Acute myocardial infarction

Plasma ANP levels are already elevated by the time patients with acute myocardial infarction are admitted to hospital and decrease thereafter. By contrast, although plasma BNP levels are significantly elevated at admission, they do not peak until 12–24 h after the onset of infarction; they then decline and peak once again 5–7 days later [57]. Furthermore, despite a gradual decline, BNP levels remain significantly elevated during the chronic phase, reflecting any permanent impairment of left ventricular function and/or remodeling that occurs. BNP levels return to normal or near normal in patients without left ventricular remodeling after successful early coronary reperfusion [58]. The height of the second peak during the acute phase serves as a valuable index of left ventricular remodeling in patients with acute myocardial infarction [59], as myocardial hypoxia, intracellular acidosis and myocardial stretch all contribute to the increase in natriuretic peptide levels during ventricular remodeling [60].

Hypertension and left ventricular hypertrophy

Several studies have shown that plasma ANP and BNP levels are higher in patients with hypertension than in normotensive individuals [61], and are higher in hypertensive patients with left ventricular hypertrophy than in those without left ventricular hypertrophy [62]. In addition, BNP levels are significantly higher in patients with left ventricular concentric hypertrophy than in those with eccentric hypertrophy or concentric remodeling, or in patients with essential hypertension but a normal left ventricular structure [63]. Antihypertensive therapy that reduces blood pressure leads to a decline in BNP levels and a reduction in left ventricular mass [64]. Measurement of BNP is also useful for detection the patients with left ventricular hypertrophy in the general population [65].

Pulmonary hypertension

Plasma ANP and BNP levels are elevated in patients with right ventricular overload, such as that caused by pulmonary hypertension, or right ventricular volume overload, such as that caused by an atrial septal defect. Interestingly, ANP is dominant in atrial septal defects [66], whereas BNP is dominant in pulmonary hypertension [67]; but when pulmonary hypertension accompanies an atrial septal defect, BNP is dominant. ANP and BNP levels correlate with mean pulmonary arterial pressure, right atrial pressure, right ventricular end-diastolic pressure and total pulmonary resistance in patients with pulmonary hypertension [67]. ANP and BNP levels decline together with a reduction in total pulmonary resistance after long-term therapy with prostaglandin derivatives [68]. Plasma BNP levels are also elevated in patients with acute pulmonary embolism. In these patients, elevated BNP is associated with right ventricular overload as well as increased mortality. Thus, pressure overload in the right atrium and ventricle stimulates ANP and BNP secretion independently of etiology, and plasma levels of these peptides are good indices of the severity and effects of treatment in patients with right ventricular overload. These results suugest that the measurement of BNP is a useful means assessing disease severity, the effect of drug treatment, and the prognosis of patients with cardiovascular disease.

Molecular complexity of BNP in plasma — increased proBNP-108 in heart failure

ProBNP-108 is thought to be cleaved to BNP-32 and N-terminal proBNP-76 in an equimolar fashion by a processing enzyme as it is secreted from ventricular myocytes. However, recent studies have shown that, in addition to NP-32 and NT-proBNP-76, proBNP-108 also circulates in human plasma and that the level of this peptide is increased in heart failure [69,70]. What is more, other studies have shown that the assay kit currently being used for BNP-32 also recognizes proBNP-108 and that there is a high degree

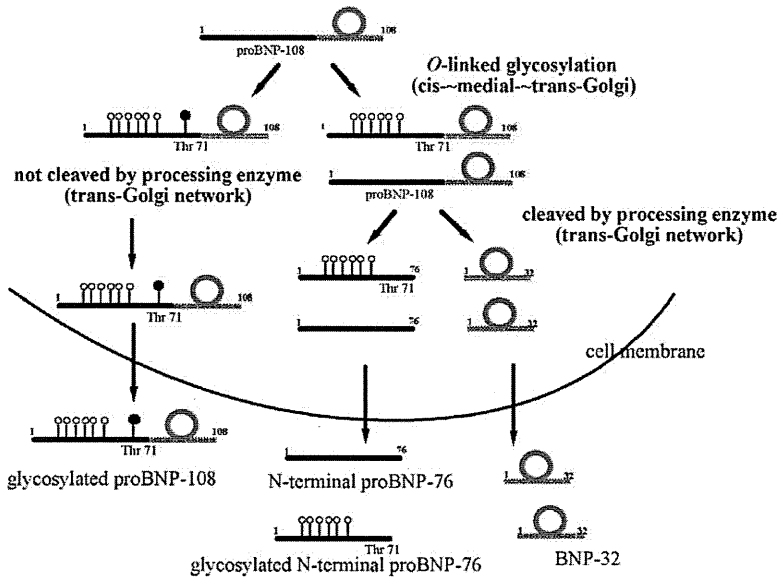

Figure 5 Schematic representation of the processing and glycosylation of proBNP in cardiomyocytes. Some of the biosynthesized proBNP-108 is *O*-glycosylated within the Golgi apparatus. If *O*-glycosylation does not occur at Thr-71, proBNP-108 is cleaved to BNP-32 and NT-proBNP-76 by furin within the trans-Golgi network. BNP-32 and NT-proBNP-76 are then secreted in an equimolar fashion. If *O*-glycosylation occurs at Thr-71 of proBNP, glycosylated-proBNP-108 is not cleaved by the processing enzyme, and uncleaved glycosylated proBNP-108 is secreted into the circulation.

of cross-reactivity [71], which suggests the BNP level measured using this assay system is the sum of the BNP-32 and proBNP-108 levels. We recently showed that both proBNP-108 and BNP-32 circulate in the plasma of patients with heart failure and that the proBNP-108/BNP-32 ratios vary greatly, depending on the patient's heart failure status [11]. This ratio is markedly higher in patients with heart failure caused by ventricular overload, as well as in those with decompensated heart failure, but the ratio is not increased in patients with atrial overload. In addition, proBNP-108 is a major molecular form in human ventricular tissue. These findings are consistent with the hypothesis that proBNP-108 is the major molecular form of BNP in the ventricle and that proBNP-108 levels increase in response to ventricular overload [11].

On the other hand, proBNP-108 does not induce cGMP production as effectively as BNP-32. In mild to moderate heart failure, the plasma cGMP level increases in proportion to the severity of the heart failure, and its level correlates with plasma BNP. In severe heart failure, however, the increases in cGMP level are attenuated relative to the disease state, so that the plasma cGMP levels no longer correlate with the BNP levels [72]. Apparently, the increase in the hormonally less active proBNP-108 that occurs in severe heart failure results in a relative deficiency in natriuretic peptide.

A new hypothesis of processing of proBNP

Recent studies have shown that proBNP-108 is *O*-glycosylated and that the degree of glycosylation depends on heart failure severity [73,74]. The clinical relevance of proBNP-108 glycosylation remains unclear, however. Various stimuli, including pressure overload, volume overload and ischemia, stimulate BNP gene transcription, after which the transcript is translated in the endoplasmic reticulum to produce preproBNP. As the protein is processed in the Golgi network, removal of its signal peptide generates proBNP-108, which can then be posttranslationally glycosylated to varying degrees at several sites in its N-terminal region (Ser36, Thr37, Thr44, Thr48, Thr53, Ser58 and Thr71). The *O*-glycosylated proBNP-108 is then transported to the trans-Golgi network, where it is cleaved to BNP-32 and NT-proBNP-76, probably by furin [75]. Both BNP-32 and NT-proBNP-76 are thought to be secreted via a constitutive pathway without storage in secretory granules.

How glyco-proBNP-108 is secreted without processing under conditions of severe heart failure is not fully understood. One recent study has shown that *O*-glycosylation at Thr-71, which is situated close to the cleavage site, impairs proBNP-108 processing by furin in HEK293 cells, a cell line derived from human embryonic kidney cells [76] (Fig. 5). Because the effect of *O*-glycosylation was only evaluated with furin in that vitro study, the actions of other potential processing enzymes are still unknown. Also unknown is whether similar glycosylation occurs in cardiac myocytes in both the atrium and ventricle. Further studies using cardiac myocytes will be required to elucidate the precise mechanism by which proBNP-108 is processed.

Conflict of interest

None of the authors have a conflict of interest.

Acknowledgements

We thank Dr. Masashi Ikeda, Dr. Kazumi Akimoto, Ms. Keiko Ishikawa, Ms. Kyoko Tabei, Ms. Masako Minato and Ms.

Machiko Sakata for their technical assistance. We thank Ms. Yukari Kubo for her excellent secretarial work.

This study was supported in part by Scientific Research Grants-in-Aid [Nos. 18590787 (to T.N.), and 20590837 (to T.N.)] from the Ministry of Education, Culture, Sports, Science and Technology of Japan, by the Science Research Promotion Fund from the Promotion and Mutual Aid Corporation for Private Schools of Japan (to T.N.), by Grants-in-Aid for Scientific Research from the Japan Society for the Promotion of Science (to K.K. and N.K.), and grants from the Japanese Ministry of Health, Labour and Welfare (to N.K.).

References

[1] Kirsch B. Electron microscopy of the atrium of the heart. Exp Med Surg 1956;14:99–112.
[2] de Bold AJ, Borenstein HB, Veress AT, Sonnenberg H. A rapid and potent natriuretic response to intravenous injection of atrial myocardial extract in rats. Life Sci 1981;28:89–94.
[3] Kangawa K, Matsuo H. Purification and complete amino acid sequence of alpha-human atrial natriuretic polypeptide. Biochem Biophys Res Commun 1984;118:131–9.
[4] Nakao K, Ogawa Y, Suga S, Imura H. Molecular biology and biochemistry of the natriuretic peptide system. I. Natriuretic peptides. J Hypertens 1992;10:907–12.
[5] Yan W, Wu F, Morser J, Wu Q. Corin, a transmembrane cardiac serine protease, acts as a pro-atrial natriuretic peptide-converting enzyme. Proc Natl Acad Sci U S A 2000;97:8525–9.
[6] Sugawara A, Nakao K, Morii N, Yamada T, Itoh H, Shiono S, et al. Synthesis of atrial natriuretic polypeptide in human failing hearts. Evidence for altered processing of atrial natriuretic polypeptide precursor and augmented synthesis of beta-human ANP. J Clin Invest 1988;81:1962–70.
[7] Akimoto K, Miyata A, Kangawa K, Koga Y, Hayakawa K, Matsuo H. Molecular forms of atrial natriuretic peptide in the atrium of patients with cardiovascular disease. J Clin Endocrinol Metab 1988;67:93–7.
[8] Sudoh T, Kangawa K, Minamino N, Matsuo H. A new natriuretic peptide in porcine brain. Nature 1988;332:78–81.
[9] Saito Y, Nakao K, Itoh H, Yamada T, Mukoyama M, Arai H, Hosoda K, Shirakami G, Suga S, Minamino N, kangawa K, Matsuo H, Imura H. Brain natriuretic peptide is a novel cardiac hormone. Biochem Biophys Res Commun 1989;158:360–8.
[10] Minamino N, Horio H, Nishikimi T. Natriuretic peptides in the cardiovascular system. In: Kastin AJ, editor. The handbook of biologically active peptides. 1st ed. New York/London: Academic Press; 2006. p. 1217–25.
[11] Nishikimi T, Minamino N, Masashi I, Takeda Y, Tadokoro K, Shibasaki I, Fukuda H, Horiuchi Y, Oikawa S, Ieiri T, Matsubara M, Ishimitsu T. Diversity of molecular forms of plasma brain natriuretic peptide in heart failure—different proBNP-108 to BNP-32 ratios in atrial and ventricular overload. Heart 2010;96:432–9.
[12] Nakayama K. Furin: a mammalian subtilisin/Kex2p-like endoprotease involved in processing of a wide variety of precursor proteins. Biochem J 1997;327:625–35.
[13] Sudoh T, Maekawa K, Kojima M, Minamino N, Kangawa K, Matsuo H. Cloning and sequence analysis of cDNA encoding a precursor for human brain natriuretic peptide. Biochem Biophys Res Commun 1989;159:1427–34.
[14] Jiang J, Pristera N, Wang W, Zhang X, Wu Q. Effect of sialylated O-glycans in pro-brain natriuretic peptide stability. Clin Chem 2010;56:959–66.
[15] Minamino N, Makino Y, Tateyama H, Kangawa K, Matsuo H. Characterization of immunoreactive human C-type natriuretic peptide in brain and heart. Biochem Biophys Res Commun 1991;179:535–42.
[16] Ogawa Y, Itoh H, Nakao K. Molecular biology and biochemistry of natriuretic peptide family. Clin Exp Pharmacol Physiol 1995;22:49–53.
[17] Gardner DG, Vlasuk GP, Baxter JD, Fiddes JC, Lewicki JA. Identification of atrial natriuretic factor gene transcripts in the central nervous system of the rat. Proc Natl Acad Sci U S A 1987;84:2175–9.
[18] Shiono S, Nakao K, Morii N, Yamada T, Itoh H, Sakamoto M, Sugawara A, Saito Y, Katsuura G, Imura H. Nature of atrial natriuretic polypeptide in rat brain. Biochem Biophys Res Commun 1986;135:728–34.
[19] Feller SM, Gagelmann M, Forssmann WG. Urodilatin: a newly described member of the ANP family. Trends Pharmacol Sci 1989;10:93–4.
[20] Mukoyama M, Nakao K, Hosoda K, Suga S, Saito Y, Ogawa Y, et al. Brain natriuretic peptide as a novel cardiac hormone in humans. J Clin Invest 1991;87:1402–12.
[21] Yasue H, Yoshimura M, Sumida H, Kikuta K, Kugiyama K, Jougasaki M, Ogawa H, Okumura K, Mukoyama M, Nakao K. Localization and mechanism of secretion of B-type natriuretic peptide in comparison with those of A-type natriuretic peptide in normal subjects and patients with heart failure. Circulation 1994;90:195–203.
[22] Kojima M, Minamino N, Kangawa K, Matsuo H. Cloning and sequence analysis of a cDNA encoding a precursor for rat C-type natriuretic peptide (CNP). FEBS Lett 1990;276:209–13.
[23] Komatsu Y, Nakao K, Suga S, Ogawa Y, Mukoyama M, Arai H, Shirakami G, Hosoda K, Nakagawa O, Hama N, Kishimoto I, Imura H. C-type natriuretic peptide (CNP) in rats and humans. Endocrinology 1991;129:1104–6.
[24] Suga S, Nakao K, Itoh H, Komatsu Y, Ogawa Y, Hama N, Imura H. Endothelial production of C-type natriuretic peptide and its marked augmentation by transforming growth factor-beta. Possible existence of "vascular natriuretic peptide system". J Clin Invest 1992;90:1145–9.
[25] Vollmar AM, Schulz R. Expression and differential regulation of natriuretic peptides in mouse macrophages. J Clin Invest 1995;95:2442–50.
[26] Minamino N, Makino Y, Tateyama H, Kangawa K, Matsuo H. Characterization of immunoreactive human C type natriuretic peptide in brain and heart. Biochem Biophys Res Commun 1991;179:535–42.
[27] Horio T, Tokudome T, Maki T, Yoshihara F, Suga S, Nishikimi T, Kojima M, Kawano Y, Kangawa K. Gene expression, secretion, and autocrine action of C-type natriuretic peptide in cultured adult rat cardiac fibroblasts. Endocrinology 2003;144:2279–84.
[28] Field LJ. Atrial natriuretic factor-SV40 T antigen transgenes produce tumors and cardiac arrhythmias in mice. Science 1988;239:1029–33.
[29] Seidman CE, Schmidt EV, Seidman JG. cis-dominance of rat atrial natriuretic factor gene regulatory sequences in transgenic mice. Can J Physiol Pharmacol 1991;69:1486–92.
[30] Knowlton KU, Rockman HA, Itani M, Vovan A, Seidman CE, Chien KR. Divergent pathways mediate the induction of ANF transgenes in neonatal and hypertrophic ventricular myocardium. J Clin Invest 1995;96:1311–8.
[31] Argentin S, Ardati A, Tremblay S, Lihrmann I, Robitaille L, Drouin J, Nemer M. Developmental stage-specific regulation of atrial natriuretic factor gene transcription in cardiac cells. Mol Cell Biol 1994;14:777–90.
[32] LaPointe MC, Wu JP, Greenberg B, Gardner DG. Upstream sequences confer atrial-specific expression on the human atrial natriuretic factor gene. J Biol Chem 1988;263:9075–8.
[33] Houweling AC, van Borren MM, Moorman AF, Christoffels VM. Expression and regulation of the atrial natriuretic factor encod-

ing gene Nppa during development and disease. Cardiovasc Res 2005;67:583–93.
[34] Debrus S, Rahbani L, Marttila M, Delorme B, Paradis P, Nemer M. The zinc finger-only protein Zfp260 is a novel cardiac regulator and a nuclear effector of alpha1-adrenergic signaling. Mol Cell Biol 2005;25:8669–82.
[35] Kuwahara K, Saito Y, Ogawa E, Takahashi N, Nakagawa Y, Naruse Y, Harada M, Hamanaka I, Izumi T, Miyamoto Y, Kishimoto I, Kawakami R, Nakanishi M, Mori N, Nakao K. The neuron-restrictive silencer element-neuron-restrictive silencer factor system regulates basal and endothelin 1-inducible atrial natriuretic peptide gene expression in ventricular myocytes. Mol Cell Biol 2001;21:2085–97.
[36] Kuwahara K, Saito Y, Takano M, Arai Y, Yasuno S, Nakagawa Y, Takahashi N, Adachi Y, Takemura G, Horie M, Miyamoto Y, Morisaki T, Kuratomi S, Noma A, Fujiwara H, et al. NRSF regulates the fetal cardiac gene program and maintains normal cardiac structure and function. Embo J 2003;22:6310–21.
[37] Tamura N, Ogawa Y, Yasoda A, Itoh H, Saito Y, Nakao K. Two cardiac natriuretic peptide genes (atrial natriuretic peptide and brain natriuretic peptide) are organized in tandem in the mouse and human genomes. J Mol Cell Cardiol 1996;28:1811–5.
[38] Ogawa Y, Itoh H, Nakagawa O, Shirakami G, Tamura N, Yoshimasa T, Nagata K, Yoshida N, Nakao K. Characterization of the 5'-flanking region and chromosomal assignment of the human brain natriuretic peptide gene. J Mol Med 1995;73:457–63.
[39] He Q, Wang D, Yang XP, Carretero OA, LaPointe MC. Inducible regulation of human brain natriuretic peptide promoter in transgenic mice. Am J Physiol Heart Circ Physiol 2001;280:H368–76.
[40] LaPointe MC, Wu G, Garami M, Yang XP, Gardner DG. Tissue-specific expression of the human brain natriuretic peptide gene in cardiac myocytes. Hypertension 1996;27:715–22.
[41] Kuwahara K, Nakao K. Regulation and significance of atrial and brain natriuretic peptides as cardiac hormones. Endocr J 2010;57:555–65.
[42] Ogawa E, Saito Y, Harada M, Kamitani S, Kuwahara K, Miyamoto Y, Ishikawa M, Hamanaka I, Kajiyama N, Takahashi N, Nakagawa O, Masuda I, Kishimoto I, Nakao K. Outside-in signalling of fibronectin stimulates cardiomyocyte hypertrophy in cultured neonatal rat ventricular myocytes. J Mol Cell Cardiol 2000;32:765–76.
[43] Ogawa E, Saito Y, Kuwahara K, Harada M, Miyamoto Y, Hamanaka I, Kajiyama N, Takahashi N, Izumi T, Kawakami R, Kishimoto I, Naruse Y, Mori N, Nakao K. Fibronectin signaling stimulates BNP gene transcription by inhibiting neuron-restrictive silencer element-dependent repression. Cardiovasc Res 2002;53:451–9.
[44] Nelson TJ, Balza Jr R, Xiao Q, Misra RP. SRF-dependent gene expression in isolated cardiomyocytes: regulation of genes involved in cardiac hypertrophy. J Mol Cell Cardiol 2005;39:479–89.
[45] Kuwahara K, Barrientos T, Pipes GC, Li S, Olson EN. Muscle-specific signaling mechanism that links actin dynamics to serum response factor. Mol Cell Biol 2005;25:3173–81.
[46] Kuwahara K, Kinoshita H, Kuwabara Y, Nakagawa Y, Usami S, Minami T, Yamada Y, Fujiwara M, Nakao K. Myocardin-related transcription factor A is a common mediator of mechanical stress- and neurohumoral stimulation-induced cardiac hypertrophic signaling leading to activation of brain natriuretic peptide gene expression. Mol Cell Biol 2010;30:4134–48.
[47] Ohta S, Shimekake Y, Nagata K. Cell-type-specific function of the C-type natriuretic peptide gene promoter in rat anterior pituitary-derived cultured cell lines. Mol Cell Biol 1993;13:4077–86.
[48] Ohta S, Shimekake Y, Nagata K. Molecular cloning and characterization of a transcription factor for the C-type natriuretic peptide gene promoter. Eur J Biochem 1996;242:460–6.
[49] Ohta S, Takeuchi M, Deguchi M, Tsuji T, Gahara Y, Nagata K. A novel transcriptional factor with Ser/Thr kinase activity involved in the transforming growth factor (TGF)-beta signalling pathway. Biochem J 2000;350(Pt 2):395–404.
[50] Burnett Jr JC, Kao PC, Hu DC, Heser DW, Heublein D, Granger JP, Opgenorth TJ, Reeder GS. Atrial natriuretic peptide elevation in congestive heart failure in the human. Science 1986;231:1145–7.
[51] Yoshimura M, Yasue H, Okumura K, Ogawa H, Jougasaki M, Mukoyama M, Nakao K, Imura H. Different secretion patterns of atrial natriuretic peptide and brain natriuretic peptide in patients with congestive heart failure. Circulation 1993;87:464–9.
[52] Wang TJ, Larson MG, Levy D, Benjamin EJ, Leip EP, Omland T, Wolf PA, Vasan RS. Plasma natriuretic peptide levels and the risk of cardiovascular events and death. N Engl J Med 2004;350:655–63.
[53] Maisel AS, Krishnaswamy P, Nowak RM, McCord J, Hollander JE, Duc P, Omland T, Storrow AB, Abraham WT, Wu AH, Clopton P, Steg PG, Westheim A, Knudsen CW, Perez A, et al. Rapid measurement of B-type natriuretic peptide in the emergency diagnosis of heart failure. Breathing Not Properly Multinational Study Investigators. N Engl J Med 2002;347:161–7.
[54] Jessup M, Abraham WT, Casey DE, Feldman AM, Francis GS, Ganiats TG, Konstam MA, Mancini DM, Rahko PS, Silver MA, Stevenson LW, Yancy CW. focused update: ACCF/AHA Guidelines for the Diagnosis and Management of Heart Failure in Adults: a report of the American College of Cardiology Foundation/American Heart Association Task Force on Practice Guidelines: developed in collaboration with the International Society for Heart and Lung Transplantation. Circulation 2009;119:1977–2016.
[55] Dickstein K, Cohen-Solal A, Filippatos G, McMurray JJ, Ponikowski P, Poole-Wilson PA, Strömberg A, van Veldhuisen DJ, Atar D, Hoes AW, Keren A, Mebazaa A, Nieminen M, Priori SG, Swedberg K, ESC Committee for Practice Guidelines (CPG). ESC Guidelines for the diagnosis and treatment of acute and chronic heart failure 2008: the Task Force for the Diagnosis and Treatment of Acute and Chronic Heart Failure 2008 of the European Society of Cardiology. Developed in collaboration with the Heart Failure Association of the ESC (HFA) and endorsed by the European Society of Intensive Care Medicine (ESICM). Task Force for Diagnosis and Treatment of Acute and Chronic Heart Failure 2008 of European Society of Cardiology. Eur Heart J 2008;29:2388–442.
[56] Heart Failure Society of America. Executive summary: HFSA 2010 comprehensive heart failure practice guideline. J Cardiac Failure 2010;16:475–539.
[57] Morita E, Yasue H, Yoshimura M, Ogawa H, Jougasaki M, Matsumura T, Mukoyama M, Nakao K. Increased plasma levels of brain natriuretic peptide in patients with acute myocardial infarction. Circulation 1993;88:82–91.
[58] Nagaya N, Goto Y, Nishikimi T, Uematsu M, Miyao Y, Kobayashi Y, Miyazaki S, Hamada S, Kuribayashi S, Takamiya M, Matsuo H, Kangawa K, Nonogi H. Sustained elevation of plasma brain natriuretic peptide levels associated with progressive ventricular remodelling after acute myocardial infarction. Clin Sci (Lond) 1999;96:129–36.
[59] Nagaya N, Nishikimi T, Goto Y, Miyao Y, Kobayashi Y, Morii I, Daikoku S, Matsumoto T, Miyazaki S, Matsuoka H, Takishita S, Kangawa K, Matsuo H, Nonogi H. Plasma brain natriuretic peptide is a biochemical marker for the prediction of progressive ventricular remodeling after acute myocardial infarction. Am Heart J 1998;135:21–8.
[60] Nishikimi T, Maeda N, Matsuoka H. The role of natriuretic peptides in cardioprotection. Cardiovasc Res 2006;69:318–28.
[61] Buckley MG, Markandu ND, Miller MA, Sagnella GA, MacGregor GA. Plasma concentrations and comparisons of brain and

atrial natriuretic peptide in normal subjects and in patients with essential hypertension. J Hum Hypertens 1993;7:245–50.
[62] Yamamoto K, Burnett Jr JC, Jougasaki M, Nishimura RA, Bailey KR, Saito Y, Nakao K, Redfield MM. Superiority of brain natriuretic peptide as a hormonal marker of ventricular systolic and diastolic dysfunction and ventricular hypertrophy. Hypertension 1996;28:988–94.
[63] Nishikimi T, Yoshihara F, Morimoto A, Ishikawa K, Ishimitsu T, Saito Y, et al. Relationship between left ventricular geometry and natriuretic peptide levels in essential hypertension. Hypertension 1996;28:22–30.
[64] Kohno M, Horio T, Yokokawa K, Yasunari K, Ikeda M, Minami M, Kurihara N, Takeda T. Brain natriuretic peptide as a marker for hypertensive left ventricular hypertrophy: changes during 1-year antihypertensive therapy with angiotensin-converting enzyme inhibitor. Am J Med 1995;98:257–65.
[65] Vasan RS, Benjamin EJ, Larson MG, Leip EP, Wang TJ, Wilson PW, Levy D. Plasma natriuretic peptides for community screening for left ventricular hypertrophy and systolic dysfunction: the Framingham heart study. JAMA 2002;288:1252–9.
[66] Nagaya N, Nishikimi T, Uematsu M, Kyotani S, Satoh T, Nakanishi N, Matsuo H, Kangawa K. Secretion patterns of brain natriuretic peptide and atrial natriuretic peptide in patients with or without pulmonary hypertension complicating atrial septal defect. Am Heart J 1998;136:297–301.
[67] Nagaya N, Nishikimi T, Okano Y, Uematsu M, Satoh T, Kyotani S, Kuribayashi S, Hamada S, Kakishita M, Nakanishi N, Takamiya M, Kunieda T, Matsuo H, Kangawa K. Plasma brain natriuretic peptide levels increase in proportion to the extent of right ventricular dysfunction in pulmonary hypertension. J Am Coll Cardiol 1998;31:202–8.
[68] Nagaya N, Nishikimi T, Uematsu M, Satoh T, Kyotani S, Sakamaki F, Kakishita M, Fukushima K, Okano Y, Nakanishi N, Miyatake K, Kangawa K. Plasma brain natriuretic peptide as a prognostic indicator in patients with primary pulmonary hypertension. Circulation 2000;102:865–70.
[69] Lam CS, Burnett Jr JC, Costello-Boerrigter L, Rodeheffer RJ, Redfield MM. Alternate circulating pro-B-type natriuretic peptide and B-type natriuretic peptide forms in the general population. J Am Coll Cardiol 2007;49:1193–202.
[70] Waldo SW, Beede J, Isakson S, Villard-Saussine S, Fareh J, Clopton P, Fitzgerald RL, Maisel AS. Pro-B-type natriuretic peptide levels in acute decompensated heart failure. J Am Coll Cardiol 2008;51:1874–82.
[71] Nishikimi T, Minamino N, Horii K, Matsuoka H. Do commercially available assay kits for B-type natriuretic peptide measure Pro-BNP1-108, as well as BNP1-32? Hypertension 2007; 50:e163.
[72] Tsutamoto T, Wada A, Maeda K, Hisanaga T, Maeda Y, Fukai D, Ohnishi M, Sugimoto Y, Kinoshita M. Attenuation of compensation of endogenous cardiac natriuretic peptide system in chronic heart failure: prognostic role of plasma brain natriuretic peptide concentration in patients with chronic symptomatic left ventricular dysfunction. Circulation 1997;96:509–16.
[73] Schellenberger U, O'Rear J, Guzzetta A, Jue RA, Protter AA, Pollitt NS. The precursor to B-type natriuretic peptide is an O-linked glycoprotein. Arch Biochem Biophys 2006;451: 160–6.
[74] Liang F, O'Rear J, Schellenberger U, Tai L, Lasecki M, Schreiner GF, Apple FS, Maisel AS, Pollitt NS, Protter AA. Evidence for functional heterogeneity of circulating B-type natriuretic peptide. J Am Coll Cardiol 2007;49:1071–8.
[75] Semenov AG, Postnikov AB, Tamm NN, Seferian KR, Karpova NS, Bloshchitsyna MN, Koshkina EV, Krasnoselsky MI, Serebryanaya DV, Katrukha AG. Processing of pro-Brain natriuretic peptide is suppressed by O-glycosylation in the region close to the cleavage site. Clin Chem 2009;55:493–8.
[76] Semenov AG, Tamm NN, Seferian KR, Postnikov AB, Karpova NS, Serebryanaya DV, Koshkina EV, Krasnoselsky MI, Katrukha AG. Processing of pro-B-type natriuretic peptide: furin and corin as candidate convertases. Clin Chem 2010;56:1166–76.

Journal of Molecular and Cellular Cardiology 50 (2011) 972–981

Contents lists available at ScienceDirect

Journal of Molecular and Cellular Cardiology

journal homepage: www.elsevier.com/locate/yjmcc

Original article

Zinc-finger protein 90 negatively regulates neuron-restrictive silencer factor-mediated transcriptional repression of fetal cardiac genes

Leo Hata [a,1], Masao Murakami [a,1], Koichiro Kuwahara [a,*], Yasuaki Nakagawa [a], Hideyuki Kinoshita [a], Satoru Usami [a], Shinji Yasuno [b], Masataka Fujiwara [a], Yoshihiro Kuwabara [a], Takeya Minami [a], Yuko Yamada [a], Chinatsu Yamada [a], Kazuhiro Nakao [a], Kenji Ueshima [b], Toshio Nishikimi [a], Kazuwa Nakao [a]

[a] Department of Medicine and Clinical Science, Kyoto University Graduate School of Medicine, Kyoto 606-8507, Japan
[b] EBM Research Center, Kyoto University Graduate School of Medicine, Kyoto 606-8507, Japan

ARTICLE INFO

Article history:
Received 19 February 2009
Received in revised form 20 January 2011
Accepted 21 January 2011
Available online 31 January 2011

Keywords:
NRSF
Zinc-finger
Transcription
Cardiac remodeling
Yeast-two hybrid
ZFP90
Fetal gene program

ABSTRACT

Neuron-restrictive silencer factor (NRSF) is a zinc-finger transcription factor that binds to specific DNA sequences (NRSE) to repress transcription. By down-regulating the transcription of its target genes, NRSF contributes to the regulation of various biological processes, including neuronal differentiation, carcinogenesis and cardiovascular homeostasis. We previously reported that NRSF regulates expression of the cardiac fetal gene program, and that attenuation of NRSF-mediated repression contributes to genetic remodeling in hearts under pathological conditions. The precise molecular mechanisms and signaling pathways via which NRSF activity is regulated in pathological conditions of the heart remain unclear, however. In this study, to search for regulators of NRSF, we carried out yeast two-hybrid screening using NRSF as bait and identified zinc-finger protein (Zfp) 90 as a novel NRSF-binding protein. NRSF and Zfp90 colocalized in the nucleus, with the zinc-finger DNA-binding domain of the former specifically interacting with the latter. Zfp90 inhibited the repressor activity of NRSF by inhibiting its binding to DNA, thereby derepressing transcription of NRSF-target genes. Knockdown of Zfp90 by siRNA led to reduced expression of NRSF-target fetal cardiac genes, atrial and brain natriuretic peptide genes, and conversely, overexpression of Zfp90 in ventricular myocardium resulted in significant increases in the expression of these genes. Notably, expression of Zfp90 mRNA was significantly upregulated in mouse and human hearts with chronic heart failure. Collectively, these results suggest that Zfp90 functions as a negative regulator of NRSF and contributes to genetic remodeling during the development of cardiac dysfunction.

1. Introduction

Chronic heart failure (CHF) is a leading cause of morbidity and mortality around the world. A key contributor to this ailment is adverse cardiac remodeling accompanied by altered expression of subsets of cardiac genes. One well-known example is the reactivation of the fetal cardiac gene program. Genes in this subset include those encoding atrial and brain natriuretic peptide (ANP and BNP, respectively), fetal type contractile proteins and fetal type ion channels, which are all abundantly expressed in fetal ventricles but become quiescent after birth. However, expression of these genes is re-induced when the heart comes under pathological stress, and is thought to play an important role in the development of cardiac dysfunction [1–3]. Thus clarification of the molecular mechanisms by which these fetal cardiac genes are regulated could lead to the identification of novel therapeutic targets for the treatment of CHF.

Neuron-restrictive silencer factor (NRSF, also known as REST) is a transcription repressor that specifically binds to 21- to 23-bp conserved DNA sequences called neuron-restrictive silencer element (NRSE, also known as RE1) [4]. Originally identified as a key regulator of neuronal gene expression and neuronal cell fate [5,6], NRSF contains a zinc-finger DNA-binding domain and two repressor domains that interact with the corepressors CoREST and mSin3, which in turn recruit methyl CpG-binding protein (MeCP) 2, histone deacetylase (HDAC), lysine-specific demethylase (LSD) 1, and other silencing/repression factors [7–18]. We previously showed that NRSF is a crucial regulator of the fetal cardiac gene program and that it is critical for proper maintenance of cardiac integrity [19,20]. For

Abbreviations: NRSE, neuron-restrictive silencer element; NRSF, neuron-restrictive silencer factor; Zfp, zinc finger protein; DBD, DNA-binding domain; CHF, chronic heart failure; ANP, atrial natriuretic peptide; BNP, brain natriuretic peptide; MeCP2, methyl CpG-binding protein2; HDAC, histone deacetylase; LSD1, lysine-specific demethylase 1; TK, thymidine kinase; DMEM, Dulbecco's modified Eagle's medium; FBS, Fetal bovine serum; MI, myocardial infarction; MHC, myosin heavy chain; SERCA, sarco/endoplasmic reticulum Ca^{2+} ATPase; RILP, REST-interacting LIM protein.

* Corresponding author at: Department of Medicine and Clinical Science, Kyoto University Graduate School of Medicine, 54, Shogoin-Kawahara-cho, Sakyo-ku, Kyoto 606-8507, Japan. Tel.: +81 75 751 4287; fax: +81 75 771 9452.
E-mail address: kuwa@kuhp.kyoto-u.ac.jp (K. Kuwahara).

[1] These authors equally contributed to this work.

0022-2828/$ – see front matter © 2011 Elsevier Ltd. All rights reserved.
doi:10.1016/j.yjmcc.2011.01.017

example, inhibition of NRSF-mediated repression in cardiac myocytes under pathological conditions leads to increased expression of ANP, a representative fetal cardiac gene [19]. In addition, cardiac-specific overexpression of a dominant-negative NRSF mutant in mouse hearts induces expression of multiple fetal cardiac genes, including those encoding ANP, BNP, skeletal α-actin, hyperpolarization-activated cyclic nucleotide-gated cation channels (HCNs) and the voltage-gated T-type Ca^{2+} channel, as well as cardiac dysfunction and sudden arrhythmic death, suggesting NRSF is necessary for normal cardiac homeostasis [20]. Moreover, we also showed that during adverse cardiac remodeling, dissociation of stress-sensitive class II HDACs from the NRSF repressor complex diminished the repressor activity of NRSF [8].

In the present study, we carried out yeast two-hybrid screening with NRSF as bait in an effort to identify other regulators of NRSF. Our results suggest that a novel NRSF binding partner, zinc-finger protein (Zfp) 90 negatively regulates NRSF, thereby contributing to the genetic remodeling that underlies adverse cardiac remodeling.

2. Materials and methods

2.1. Plasmid construction

Plasmids encoding NRSF was described previously [19]. cDNA encoding full length Zfp90 was amplified by PCR using a mouse E10.5 cDNA library as template. After confirming the sequence, cDNA was introduced into pcDNA 3.1-myc, pcDNA 3.1-flag and pCMV-DB vector for expression. Deletion mutants of NRSF and Zfp90 were all generated by PCR and inserted into myc-, flag- and Gal4-DNA binding domain (DBD)-tagged expression vectors. The NRSE-TK-luc and mutNRSE-TK-luc series were made by introducing a fragment of the minimal thymidine kinase (TK) promoter and double stranded oligonucleotides containing the NRSE or mutant NRSE sites from the BNP promoter into pGL4.10 (Promega). G5-TK-luc was made by introducing a fragment containing five Gal4-binding sites upstream of the TK promoter into pGL4.10 (Promega). BNP-luc and mutBNP-luc were constructed by inserting −1823 bp from the 5′ flanking region of the human BNP gene (bps −1823 to +98), including the intact (BNP-luc) or mutated (mutBNP-luc) NRSE sequence, upstream of a luciferase reporter gene in pGL3 vector, as described previously [21].

2.2. Yeast two-hybrid screening

A fragment of NRSF DNA-binding domain (145–418) containing multiple zinc finger motifs (NRSF-DBD) was inserted into pGBK-T7 vector for bait constructs. Yeast two-hybrid screening was carried out according to the manufacturer's (Clontech) protocol using NRSF-DBD as bait with a cDNA library from whole mouse embryo (E10.5). Positive clones were selected based on growth in selection media lacking leucine, tryptophan, histidine and adenine, and through detection of β-galactosidase activity. The plasmids in positive yeast clones were recovered, cloned into *E. coli* and then sequenced.

2.3. Cell culture and reporter assays

293T and Cos7 cells were maintained in Dulbecco's modified Eagle's medium (DMEM) supplemented with 10% fetal bovine serum (FBS) and antibiotics at 37 °C under 5% CO_2. Transfection was carried out using Fugene 6 reagent (Roche).

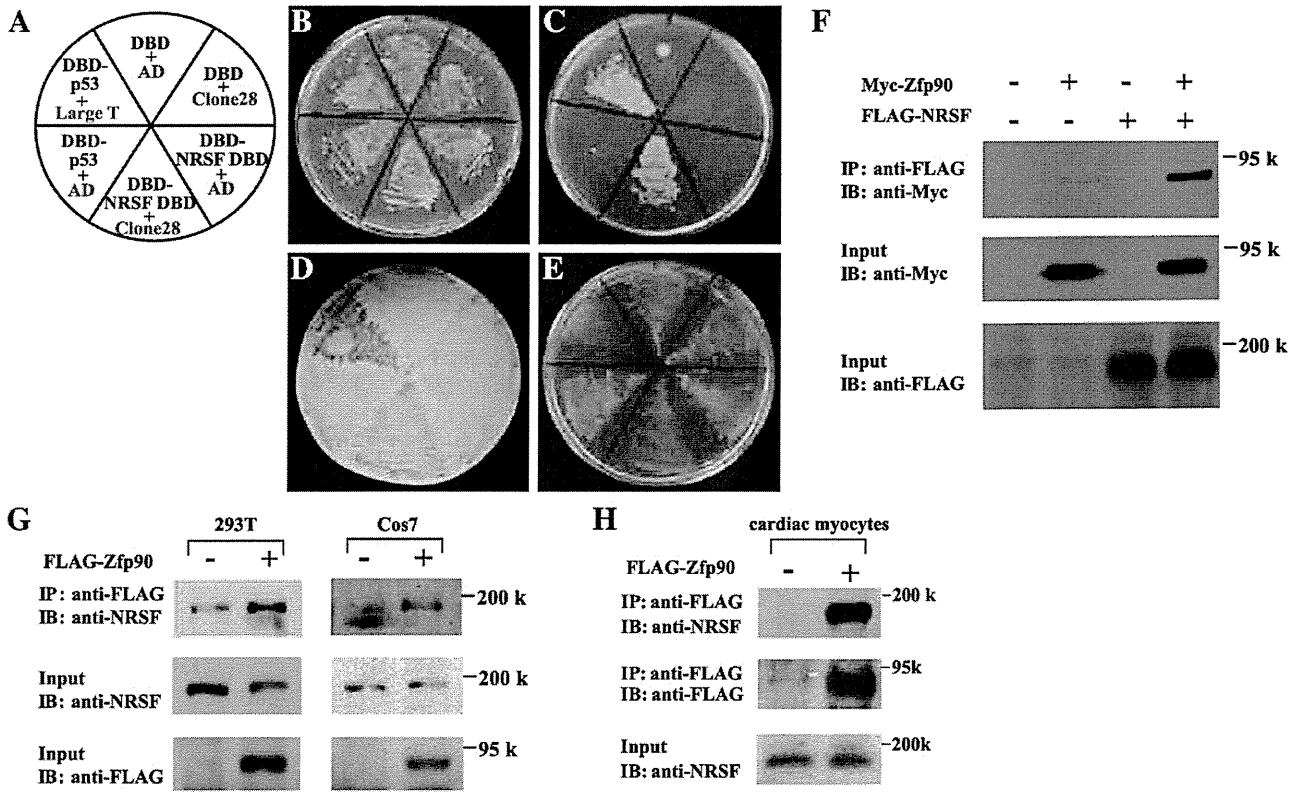

Fig. 1. Identification of Zfp90 as a NRSF binding partner. A–E, Yeast expressing each bait and prey were gown on a plate with SD-Leu-Trp (B) or SD-Leu-Trp-His-Ade (C). β-lacZ (D) and α-lacZ (E) assays were carried out to confirm the interaction. The combination of p53 and SV40 T antigen served as a positive control. F, Co-immunoprecipitation experiments were performed using FLAG-NRSF and Myc-Zfp90 expressed in 293T cells (upper). NRSF was immunoprecipitated (IP) using anti-FLAG antibody followed by immunoblotting (IB) using anti-Myc antibody (upper panel). Expression of each protein was analyzed by immunoblotting (input; lower two panels). G and H, Zfp90 associated with endogenous NRSF in 293T and Cos7 cells (G) as well as cultured neonatal ventricular myocytes (H). FLAG-Zfp90 was expressed in 293T and Cos7 cells as indicated above, after which Zfp90 was immunoprecipitated using anti-FLAG antibody followed by immunoblotting using anti-NRSF antibody (upper panel). Expression of each protein was also analyzed by immunoblotting (input).

2.4. Ventricular myocyte culture and transfection

Neonatal rat ventricular myocytes were prepared on a Percoll gradient, after which their transient transfection was carried out using Fugene 6 reagent (Roche), as previously described [19,22,23].

2.5. Gel shift assay

The procedure for gel shift analysis was described previously [19]. Nuclear extracts were prepared from 293T cells expressing Flag-NRSF or Myc-Zfp90, and the proteins' expression was confirmed by Western blotting. Initially, double stranded oligonucleotide probes were end-labeled with biotin. The binding reaction was carried out for 30 min at room temperature, after which the samples were applied to 5% native PAGE. The probes were then transferred onto nylon membranes, and the signals were detected using HRP-conjugated avidin (PIERCE). Under modified conditions, the DNA-protein complex was cross-linked with 1% formaldehyde for 10 min, and then glycine was added to stop the reaction prior to running the native PAGE.

2.6. Quantitative RT-PCR analysis

Using Trizol reagent (Invitrogen), total RNA was prepared from mouse cardiac ventricles subjected to sham operation ($n=6$) or myocardial infarction (MI) ($n=4$), from cardiac ventricles of cardiac specific Zfp90 transgenic mice (Zfp90-Tg) ($n=3$) or control wild type littermates ($n=3$), and from human hearts (left ventricles) with CHF or healthy hearts (normal; $n=5$, chronic heart failure; $n=5$). Real-time-RT-PCR was carried out using 10 ng of total RNA with TaqMan One-Step RT-PCR Mix reagent according to the manufacturer's protocol (Applied Biosystems). The mRNA expression of each gene of interest was normalized to that of the corresponding 18S and then shown as a relative mRNA level.

2.7. Mouse model of MI

MI was induced in male C67BL/6J mice (age, 8 to 12 weeks; weight, 25 to 30 g) by ligation of the left coronary artery as described previously [24].

2.8. Human tissue samples

Frozen samples of left ventricular tissue from the hearts of individuals diagnosed with CHF (5 males; average age 56.4 years; 3 hearts with ischemic cardiomyopathy, 1 heart with valvular heart disease and 1 heart with idiopathic cardiomyopathy) or healthy hearts (3 males and 2 females; average age 43.8 years) were obtained at Kyoto University Hospital. This study involves the use of existing pathological specimens, and the information was recorded in such a manner that the subjects cannot be identified directly or through identifiers linked to the subjects. This study was conducted in

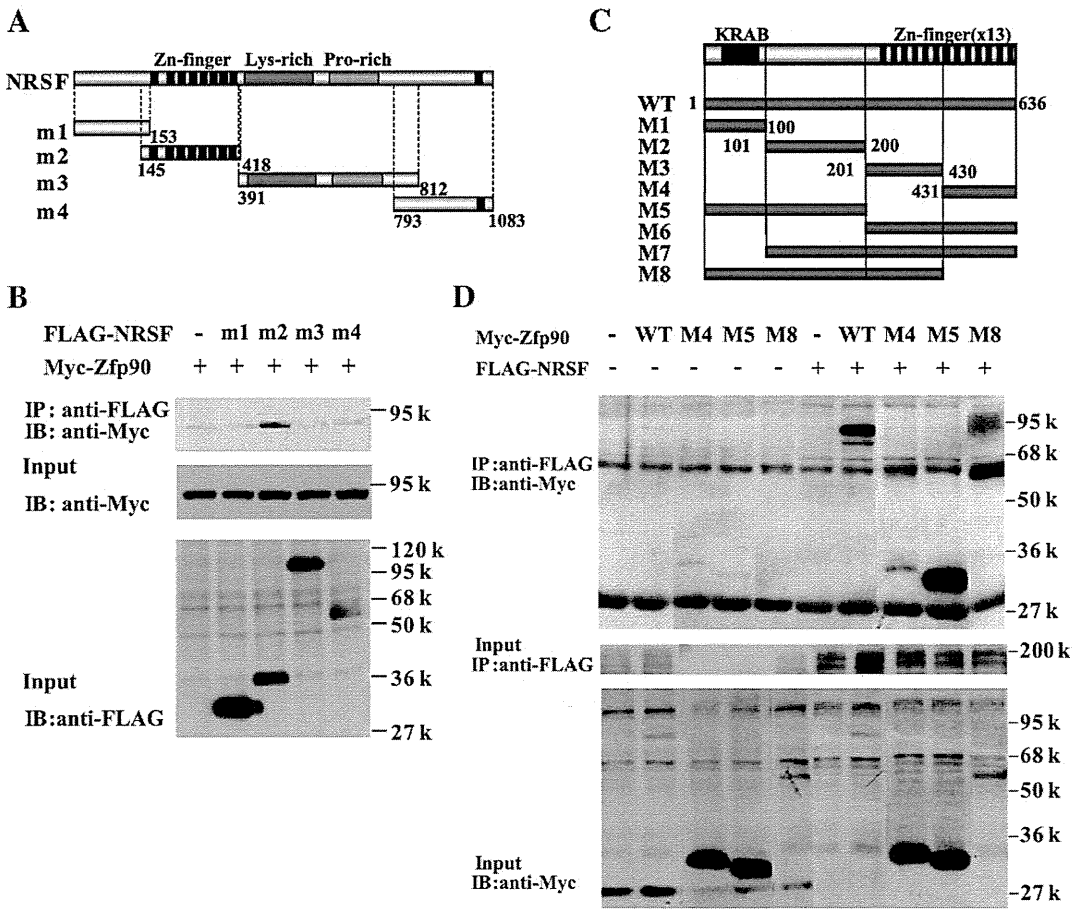

Fig. 2. Determination of the interaction domains of NRSF and Zfp90. A, Schematic diagram showing the structures of mouse NRSF and its deletion mutants. B, Co-immunoprecipitation using FLAG-tagged NRSF mutants and Myc-Zfp90 expressed in 293T cells (upper) was performed. Expression of each protein was analyzed by immunoblotting (input; middle and lower panels). C, Schematic diagram showing the structures of mouse Zfp90 and its deletion mutants. D, NRSF was immunoprecipitated (IP) using anti-FLAG antibody followed by immunoblotting (IB) using anti-Myc antibody. Expression of each protein was analyzed by immunoblotting (input).

accordance with the institutional guidelines of Kyoto University Hospital. The investigation conforms to the principles outlined in the Declaration of Helsinki.

2.9. Generation of α-MHC-flag-Zfp90 transgenic mice

A mouse Zfp90 cDNA along with a 5′-flag epitope tag was cloned into the *SalI* site of pBluescript αKS(+) plasmid containing the α-myosin heavy chain (MHC) promoter. The resultant α-MHC-flag-Zfp90 transgenic construct was then released from the vector backbone by digestion with *NotI* and purified for injection into the pronucleus of fertilized oocytes harvested from C57BL/6J mice. The surviving embryos were then transferred to the oviducts of pseudo-pregnant MCH mice.

2.10. Statistical analysis

Data are presented as means ± SEM. Unpaired *t*-tests were used for comparisons between two groups, and ANOVA with post hoc Fisher tests were used for comparisons among groups. Values of $P<0.05$ were considered significant.

3. Results

3.1. Identification of Zfp90 as a NRSF binding partner

Using NRSF-DBD as bait, we screened about 3 million clones from an E10.5 mouse cDNA library for novel interacting partners. One hundred twenty-two positive clones were obtained in the first screening based on growth selection, followed by a second screening based on detection of β-galactosidase activity. By analyzing the sequence of each clone, we identified 14 candidate NRSF-binding molecules based on whether the clones were predicted to be nuclear factors or signaling molecules (e.g., protein kinases) that might modulate NRSF function. One of the positive clones (clone 28) encoded the C-terminal 272 amino acids (365–636) of Zfp90, a zinc-finger protein also containing a KRAB domain. The interaction between this clone and NRSF-DBD in yeast was confirmed by the finding that yeast expressing NRSF-DBD and clone 28 grew well in the absence of Leu, Trp, His and Ade (Fig. 1A, B and C). The interaction between NRSF-DBD and clone 28 was also confirmed in an assay examining β- and α-galactosidase activities in yeast (Fig. 1D and E).

To determine whether Zfp90 physically interacts with NRSF in mammalian cells, we cloned full-length Zfp90 and then carried out a set of co-immunoprecipitation assays. After coexpressing Myc-Zfp90 and FLAG-NRSF in 293T cells, NRSF was immunoprecipitated using anti-FLAG antibody and then immunoblotted with anti-Myc antibody to confirm its binding to Zfp90 (Fig. 1F). We also assessed the interaction between Zfp90 and endogenous NRSF in 293T and Cos7 cells. As shown in Fig. 1G, both cell types endogenously expressed NRSF, which was co-immunoprecipitated with Zfp90, suggesting Zfp90 physically interacts with NRSF in mammalian cells. Likewise, Zfp90 physically interacted with endogenous NRSF in cultured cardiac ventricular myocytes (Fig. 1H).

To identify the interacting domain, we repeated the co-immunoprecipitation experiments using a set of NRSF deletion mutants (Fig. 2A). We first found that the DNA binding domain of NRSF is the site that specifically interacts with Zfp90, which is consistent with the results of the initial yeast two hybrid screening (Fig. 2B). The N-terminal and C-terminal repressor domains of NRSF did not interact with Zfp90 (Fig. 2B). Then using a set of Zfp90 deletion mutants, we found that the N-terminal region of Zfp90 strongly associates with NRSF (Fig. 2C and D). The C-terminal region of Zfp90 (M4), which initially appeared to bind to NRSF in yeast two-hybrid screening, also showed an interaction with NRSF (Fig. 2D). We therefore conclude that Zfp90 interacts with NRSF via both its N- and C-terminal regions. Note that some Zfp90 deletion mutants (M1, 2, 3, 6 and 7) were not stably expressed in the cells, so we could not more precisely determine the Zfp90 interaction domain (Fig. 2D). What is more, immunostaining carried out after co-expression of myc-NRSF and FLAG-Zfp90 in COS7 cells clearly showed that NRSF and Zfp90 colocalize exclusively in the nucleus (Fig. 3).

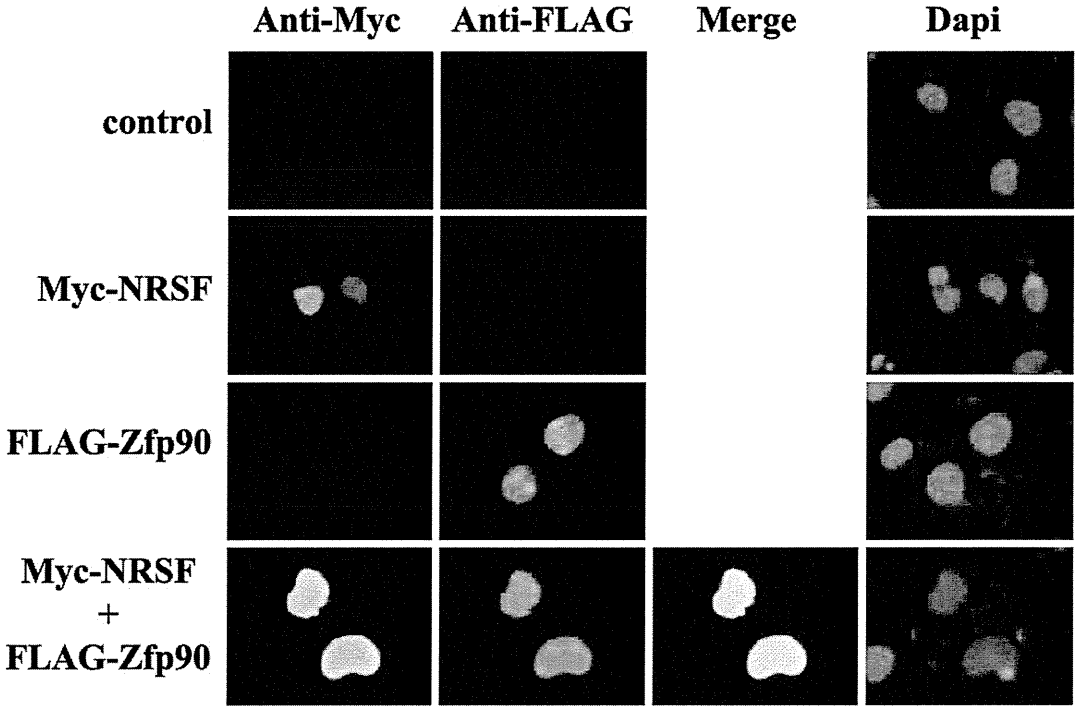

Fig. 3. Subcellular localization of NRSF and Zfp90 in cultured cells. Immunocytochemical analysis of Cos7 cells transfected with Myc-NRSF and FLAG-Zfp90 is shown. NRSF and Zfp90 were respectively detected using anti-Myc antibody with Alexa Fluor 488 (green)-labeled anti-rabbit antibody and anti-FLAG antibody with Alexa Fluor 594 (red)-labeled anti-mouse antibody.

3.2. Zfp90 inhibits the repressor activity of NRSF

We assessed the effects of Zfp90 on the repressor activity of NRSF using a set of NRSF-responsive reporters. The NRSE sequence from the human BNP promoter or its mutated sequence was inserted, in tandem, into the pGL4.10-TK-luc reporter plasmid (Fig. 4A). As shown in Fig. 4B, each reporter containing the intact NRSE sequence (left panel) exhibited less luciferase activity than those with the mutated NRSE sequences (right panel). The level of reporter activity was completely dependent on the number of NRSE sequences, and overexpression of NRSF further repressed reporter activity controlled by intact NRSEs in a dose-dependent manner (Fig. 4B, left panel). We next used siRNA to assess the specificity of these reporters for NRSF and rule out the possibility that other endogenous factors, including unidentified NRSF-like or NRSF family proteins, affect NRSE-dependent transcriptional repression. Seventy-two hours after transfecting 293T cells with siRNA targeting human NRSF, the expression of endogenous NRSF was almost completely blocked (Fig. 4C). Under the same conditions, the repressor activity of intact NRSE sequences was diminished almost to the level seen with the mutated NRSE sequences (Fig. 4D), indicating that the reporter system we established was very sensitive and specific for NRSF.

Using this reporter system, we examined the effect of Zfp90 on NRSF repressor activity. As shown in Fig. 4E, Zfp90 partially, but significantly, inhibited the transcriptional repression mediated by NRSF. When NRSF was co-expressed exogenously, Zfp90 strongly and significantly inhibited NRSE-mediated repression (Fig. 4E). On the other hand, Zfp90 showed no significant repressive effect on the

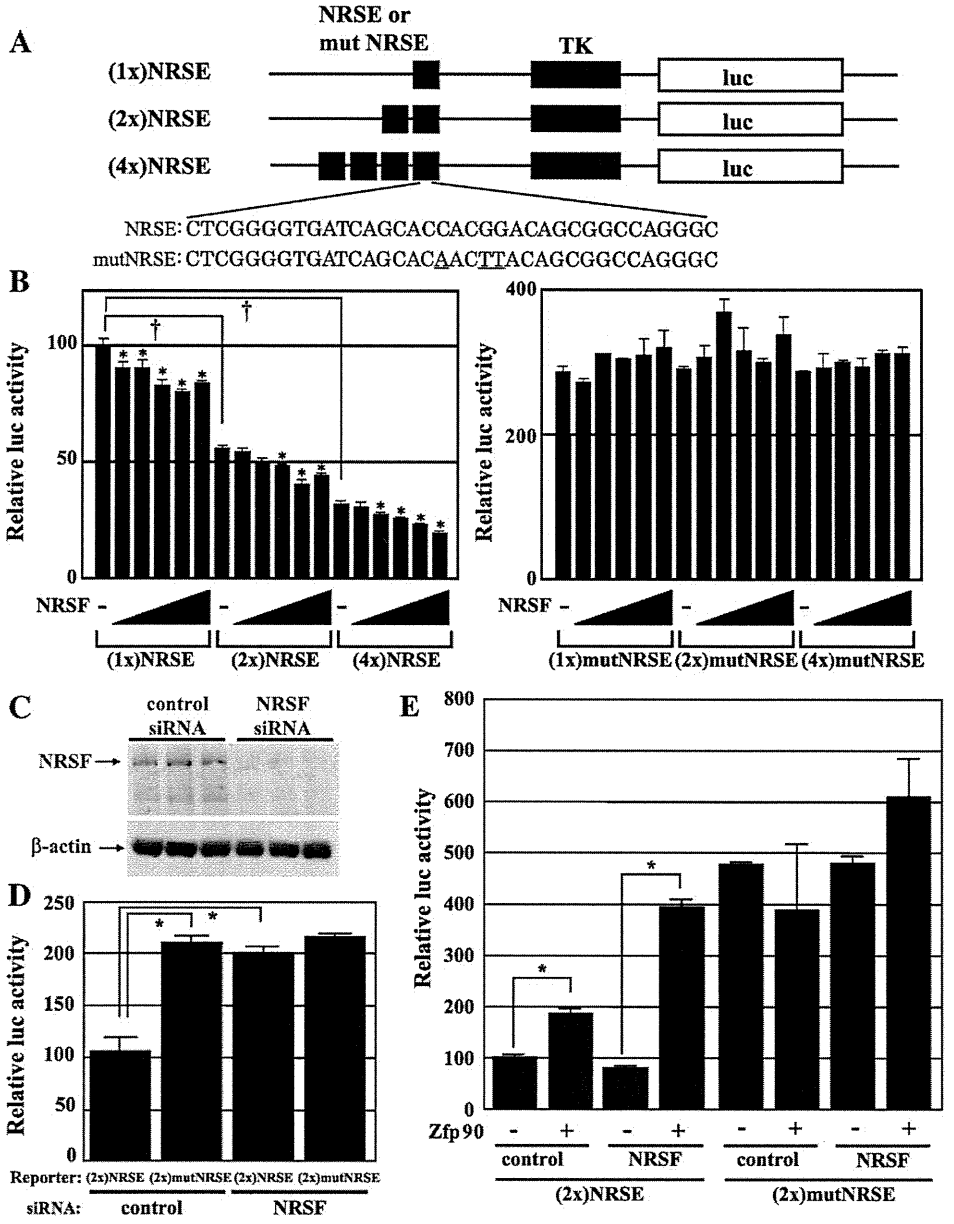

Fig. 4. Zfp90 attenuates the repressor activity of NRSF. A, Schematic diagram showing the structures of the NRSE or mutNRSE reporter constructs. Intact or mutated NRSE was introduced upstream of the TK promoter and luciferase gene. B, An NRSF expression plasmid (0, 0.3, 1, 3, 10, 30 ng) along with each NRSE (left panel) or mutNRSE (right panel) reporter (200 ng) and RSV-lacZ (50 ng) were cotransfected into 293T cells, after which luciferase activity was assayed. *$P<0.05$ vs. NRSF(−) in each reporter group. †$P<0.05$. C, siRNA targeting human NRSF (100 nM) or nonspecific control siRNA (100 nM) was transfected into 293T cells, after which expression of endogenous NRSF was analyzed by immunoblotting using anti-NRSF antibody (upper panel). The lower panel is a loading control (β-actin). D, siRNA targeting human NRSF (100 nM) was cotransfected along with a reporter plasmid into 293T cells, after which luciferase activity was assayed. *$P<0.05$. E, NRSF (10 ng) and Zfp90 (150 ng) were cotransfected into 293T cells together with a reporter construct (100 ng), after which luciferase activity was assayed. *$P<0.05$. All graphs show means ± SEM.

activity of promoters with mutated NRSE sequences (Fig. 4E), demonstrating that the effect of Zfp90 was specific to NRSF. Zfp90 thus appears to function as a negative regulator of NRSF.

3.3. Zfp90 inhibits DNA binding of NRSF

Given that Zfp90 binds to NRSF-DBD, we assessed the degree to which Zfp90 inhibits NRSF repressor activity by altering its DNA binding activity. In gel shift assays using a DNA probe containing the NRSE from the BNP promoter, a shifted band reflecting NRSF binding to the NRSE sequence was readily detected, as we have previously reported (Fig. 5A, lane 2) [21]. Moreover, this shifted band was eliminated in the presence of an excess of unlabeled competitor, but not in the presence of a mutant competitor (Fig. 5A, lanes 3 and 4). Zfp90 did not bind to the NRSE sequence at all (Fig. 5A, lane 8), indicating that Zfp90 does not compete with NRSF for the NRSE sequence.

Because the effects of Zfp90 on NRSF binding to DNA were not completely clear in the standard gel shift protocols, we attempted to increase the sensitivity of the assay by cross-linking the DNA-protein complex using formaldehyde and then applying the complex to the gel. Under these conditions, the shifted band containing the NRSF-DNA complex was weaker in the presence of Zfp90 than that in its absence, which indicates Zfp90 inhibits NRSF binding to DNA (Fig. 5B). Consistent with that notion, no supershifted band, which would indicate the presence of a NRSF-Zfp90-DNA complex and would be observed above the shifted band, was detected (Fig. 5B).

We also performed ChIP assays to further confirm that Zfp90 inhibits DNA-binding of NRSF in cardiac myocytes. We found that recruitment of NRSF to NRSE within the BNP 5′-flanking region was inhibited by overexpression of Zfp90 in cardiac myocytes (Fig. 5C). We then assessed the effect of Zfp90 on NRSF-mediated transcriptional repression in cardiac myocytes. As shown in Fig. 5D, overexpression of Zfp90 significantly inhibited NRSF-mediated repression of BNP promoter activity in cardiac myocytes. Conversely, knocking down Zfp90 in cardiac myocytes resulted in a further reduction in the activity of the BNP promoter containing intact NRSE, whereas it had no effect on the activity of a BNP promoter containing mutant NRSE (Fig. 5E). All these results demonstrate that Zfp90 inhibits NRSF-mediated transcriptional repression by inhibiting the DNA-binding of NRSF in cardiac myocytes.

Our results show that Zfp90 inhibits the repressor activity of NRSF by binding to NRSF DBD, while Zfp90 reportedly acts as a transcriptional repressor when recruited to gene regulatory regions [25]. We therefore used a Gal4-fusion system to test the possibility that Zfp90 has a transcription activation domain. Several Zfp90 deletion mutants (Fig. 2C) were separately fused to the Gal4 DNA-binding domain and transfected into 293T cells together with the G5-

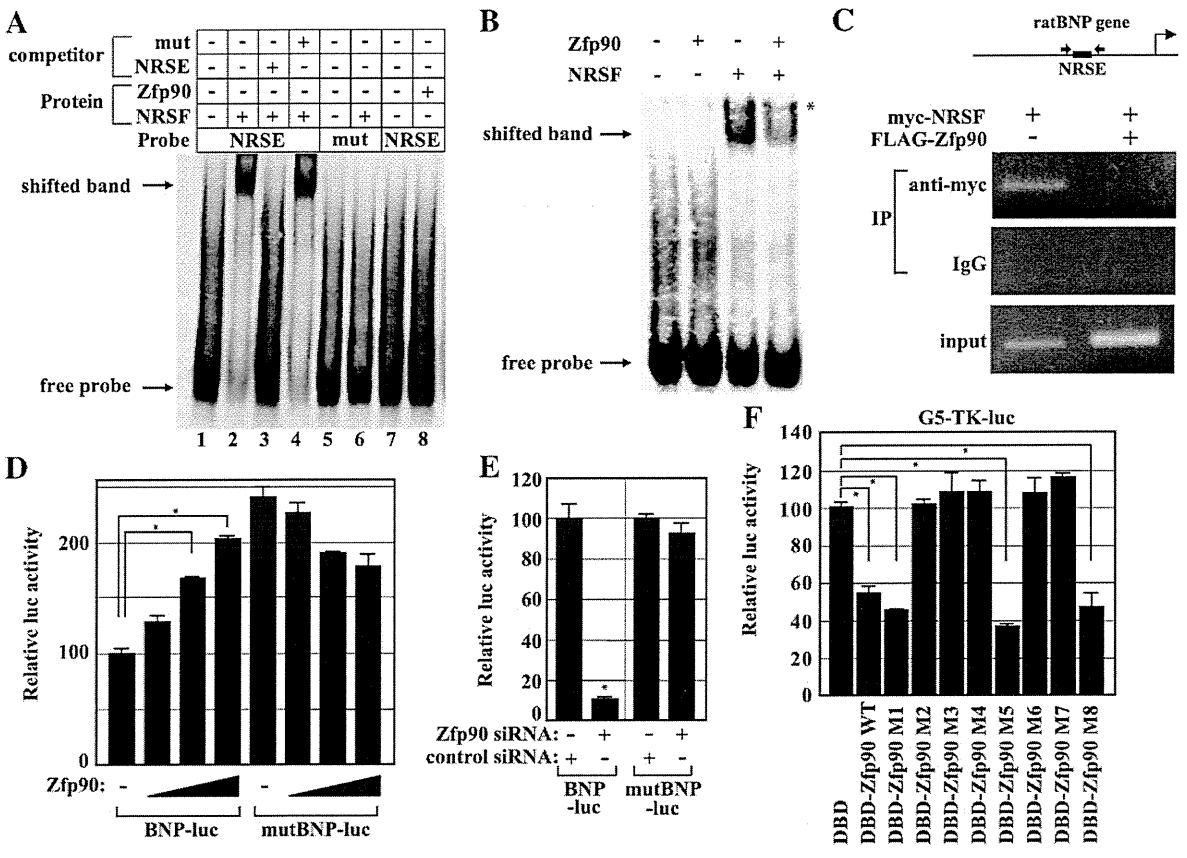

Fig. 5. Zfp90 inhibits the DNA binding activity of NRSF. A, Gel shift assays carried out using nuclear extracts from 293T cells expressing NRSF or Zfp90 and a biotin-labeled DNA probe containing NRSE sequences. Competition assays were carried out using an excess (100×) of unlabeled NRSE probe or its mutated form. B, Modified gel shift assay carried out using lysates from cells expressing NRSF and/or Zfp90, as indicated above, and a DNA probe containing NRSE. After incubation, the DNA-protein complex was cross-linked with formaldehyde, which was followed by 5% native PAGE. The asterisk (*) indicates the wells of the gel. C, ChIP assay carried out with cultured ventricular myocytes transfected with myc-NRSF and FLAG-Zfp90 using anti-myc antibody. PCR was performed with chromatin from around the NRSE in the BNP promoter region. Aliquots of chromatin obtained before immunoprecipitation were also analyzed as input. Representative PCRs with identical results in three independent experiments are shown. Schematic representations of the location of the PCR primers in the BNP gene are shown in the upper panel. D, Ventricular myocytes were cotransfected with BNP-luc or mutBNP-luc (200 ng) and an expression vector encoding Zfp90 (0, 10, 30, 100 ng). *$P<0.05$. E, Ventricular myocytes were cotransfected with Zfp90 siRNA or control siRNA (200 nM each) and BNP-luc or mutBNP-luc (100 ng each). *$P<0.05$ vs. control siRNA in each group. F, Wild-type Zfp90 and its deletion mutants (Fig. 2C) were fused to the Gal4 DNA binding domain (DBD). DBD-Zfp90 and its deletion mutants (10 ng) along with 5× UAS-luciferase reporter, G5-TK-luc (100 ng) and RSV-lacZ (10 ng) were cotransfected into 293T cells, after which reporter activity was estimated in luciferase assays. *$P<0.05$. All graphs show means ± SEM.

TK-luc reporter plasmid. As shown in Fig. 5F, Zfp90-M1, -M5 and -M8, as well as full-length Zfp90, all exhibited significant repressor activity. Notably, these deletion mutants and the full-length protein all contained a KRAB domain, suggesting the KRAB domain is the repressor domain of Zfp90. In contrast, there was no transcription activation domain detected in Zfp90.

3.4. Zfp90 modulates the expression of NRSF-regulated fetal cardiac genes

We then assessed the contribution made by Zfp90 to the regulation of endogenous fetal cardiac gene expression. Knocking down Zfp90 using siRNA in cultured ventricular myocytes significantly reduced the expression of the NRSF-targeted fetal cardiac genes ANP, BNP and HCN4, without affecting the expression of the sarco/endoplasmic reticulum Ca^{2+} ATPase (SERCA) 2 gene (Fig. 6A), which strongly supports our notion that Zfp90 inhibits NRSF-mediated transcriptional repression of some fetal cardiac genes. In addition, to evaluate the effect of overexpressing Zfp90 on expression of these genes in cardiac myocytes, we generated transgenic mice overexpressing Zfp90 in a cardiac-specific manner using α-MHC promoter (Zfp90-Tg). We compared the expression of ANP, BNP, HCN4 and SERCA2 genes between 12-week-old Zfp90-Tg and their control wild-

Table 1
Body weight, heart weight, lung weight, blood pressure, heart rate and echocardiographic data in WT and Zfp90-Tg mice.

	WT	Tg
Body weight (g)	30.3 ± 0.2	29.7 ± 1.1
Heart weight (g)	0.14 ± 0.01	0.14 ± 0.01
Lung weight (g)	0.15 ± 0.01	0.16 ± 0.01
HW/BW (mg/g)	4.6 ± 0.1	4.7 ± 0.1
LW/BW (mg/g)	5.0 ± 0.1	5.4 ± 0.2
Hemodynamic data		
Blood pressure (mmHg)	108.3 ± 2.2	108.0 ± 1.0
Heart rate (/min)	651.3 ± 27.7	621.8 ± 28.6
Echocardiographic Data		
LVDd (mm)	3.1 ± 0.1	3.0 ± 0.1
LVDs (mm)	1.7 ± 0.1	1.6 ± 0.1
EF (%)	82.0 ± 2.4	83.0 ± 1.9
FS (%)	44.5 ± 2.6	45.5 ± 2.1
IVS (mm)	0.93 ± 0.04	0.83 ± 0.04
PW (mm)	0.95 ± 0.02	0.98 ± 0.04

Values are means ± SEM. HW/BW, heart weight to body weight ratio; LW/BW, lung weight to body weight ratio; LVDd, left ventricular diastolic dimension; LVDs, left ventricular systolic dimension; EF, ejection fraction; FS, fractional shortening; IVS, intraventricular septum wall thickness; PW posterior wall thickness. $N=4$ in WT and 4 in Tg. There are no significant differences among the data between WT and Tg.

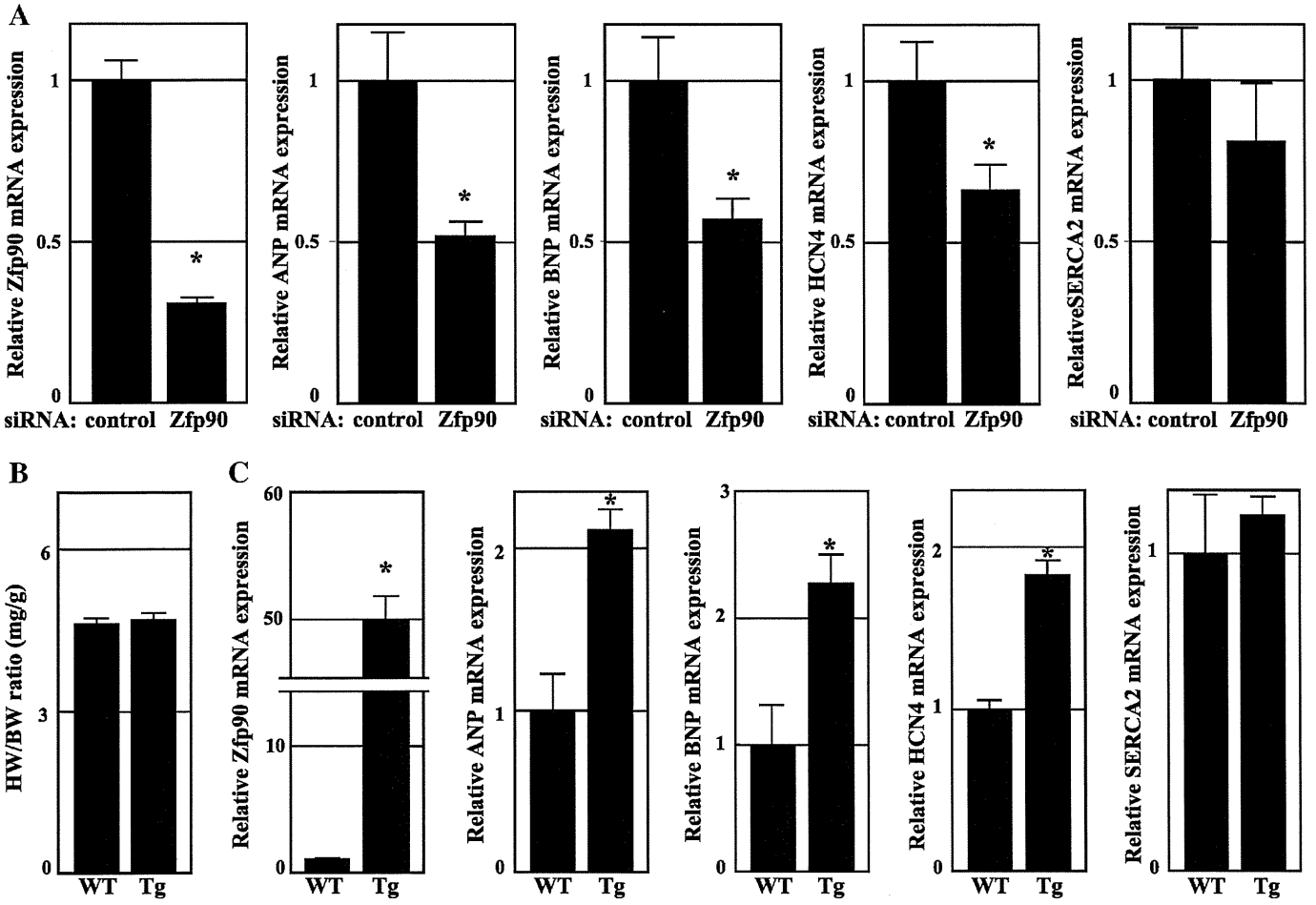

Fig. 6. Zfp90 modulates expression of NRSF-target fetal cardiac genes in cardiac myocytes. A, Zfp90, ANP, BNP, HCN4 and SERCA2 gene expression in cultured ventricular myocytes treated with Zfp90 siRNA or control siRNA was assessed by real-time RT-PCR. $n=4$ each. The relative gene expression in myocytes transfected with control siRNA was assigned a value of 1.0. Graphs show means ± SEM. *$P<0.05$ vs. control. B, Heart weight-to-body weight (HW/BW) ratios in cardiac-specific Zfp90-Tg mice (Tg) and their control wild-type littermates (WT). C, Relative levels of Zfp90, ANP, BNP, HCN4 and SERCA2 gene expression in ventricles from 12-week-old Zfp90-Tg (Tg) mice were assessed by real-time RT-PCR. $n=3$ each. The relative gene expression in cardiac ventricles from control wild-type littermates (WT) was assigned a value of 1.0. Graphs show means ± SEM. *$P<0.05$ vs. wild-type mice.

type littermates. There was no obvious difference in cardiac morphology or function evaluated based on heart weight-to-body weight ratios and echocardiography (Fig. 6B and Table 1). As shown in Fig. 6C, the expression of ANP, BNP and HCN4 genes, which are NRSF-target fetal cardiac genes, was significantly higher in Zfp90-Tg ventricles than control wild-type ventricles, while the expression of SERCA2 expression did not significantly differ between them (Fig. 6C). These findings suggest that Zfp90 participates to the regulation of the expression of some fetal cardiac genes through the attenuation of NRSF-mediated repression.

3.5. Increased expression of Zfp90 mRNA in failing hearts

Given Zfp90's ability to inhibit NRSF repressor activity and the increased expression of NRSF target genes such as BNP seen during adverse cardiac remodeling [19,20], we tested whether Zfp90 expression might be upregulated in failing hearts. As shown in Fig. 7A and B, Zfp90 gene expression was significantly increased in mouse hearts 28 days after induction of MI, a time when BNP gene expression was also significantly induced. In addition, the gene expression of both Zfp90 and BNP was dramatically increased in failing human ventricles, as compared to healthy controls (Fig. 7C and D). Taken together, these results suggest Zfp90 is importantly involved in the genetic remodeling that underlies the development of heart failure.

4. Discussion

We previously reported that NRSF regulates the transcription of multiple fetal cardiac genes, that attenuation of NRSF-mediated repression contributes to the increased cardiac expression of these genes under pathological conditions, and that this derepression plays an important role in molecular pathways leading to adverse cardiac remodeling [19,20]. Indeed, cardiac-specific overexpression of a dominant-negative form of NRSF in mice induced reactivation of the fetal cardiac gene program, cardiac dysfunction and sudden arrhythmic death, suggesting NRSF is crucial for maintaining normal cardiac homeostasis [20]. In an effort to clarify the regulatory pathways governing NRSF activity, we used yeast two-hybrid screening with NRSF as bait and identified Zfp90 as a novel NRSF-binding protein. NRSF and Zfp90 colocalized in the nucleus, and the DNA-binding zinc-finger domain of NRSF specifically interacted with Zfp90. Zfp90 inhibited the repressor activity of NRSF by blocking its binding to DNA, thereby weakening NRSF-mediated repression of target genes expression. Furthermore, expression of Zfp90 mRNA was significantly upregulated in mouse hearts with MI and in human hearts with CHF, and in both cases expression of NRSF-target genes was upregulated. Collectively, these findings suggest that Zfp90 functions as a negative regulator of NRSF and contributes to the genetic remodeling underlying the development of cardiac dysfunction (Fig. 7E).

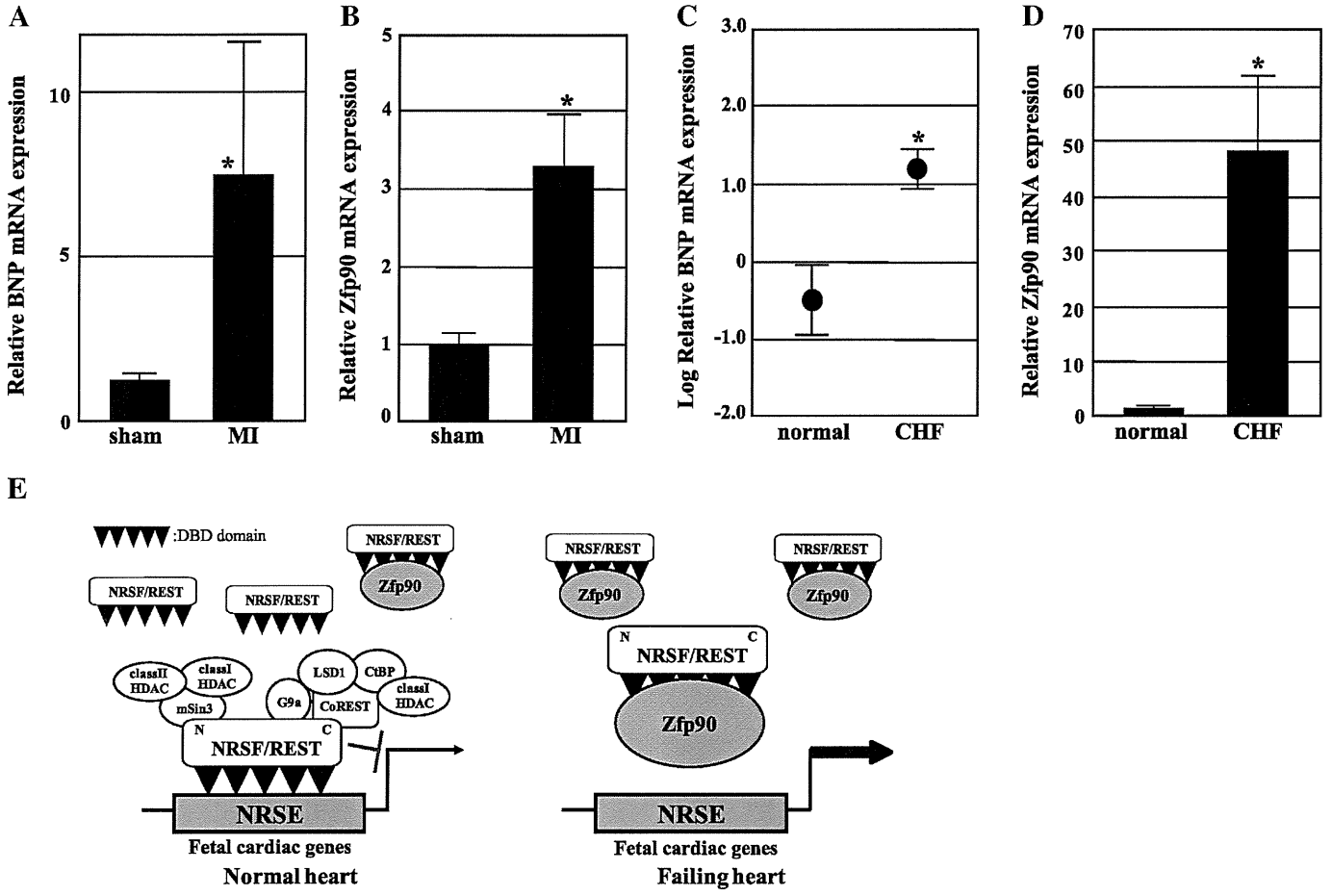

Fig. 7. Increase in the cardiac expression of Zfp90 mRNA in mice subjected to myocardial infarction and in human CHF. A and B, Using real time RT-PCR, expression of BNP (A) and Zfp90 (B) mRNA was assessed in mice 28 days after sham operation (sham) or induction of myocardial infarction (MI) (sham, $n=6$; MI, $n=4$). *$P<0.05$ vs. sham operation. The relative mRNA level in sham-operated mice was assigned a value of 1.0. Graphs show means ± SEM. C and D, Using real time PCR, expression of BNP (A) and Zfp90 (B) mRNA was assessed in healthy (normal) and failing (CHF) human hearts (normal, $n=5$; CHF, $n=5$). *$P<0.01$ vs. normal hearts. The relative mRNA level in normal hearts was assigned a value of 1.0. Y-axis in panel C is the log relative BNP mRNA expression. Graphs show means ± SEM. E, Schematic representation of our conclusion drawn from the findings of this study. Zfp90 inhibits NRSF-mediated transcriptional repression of fetal cardiac gene transcription and may contribute to genetic reprogramming during the development of heart failure. N: N-terminal repressor domain of NRSF. C: C-terminal repressor domain of NRSF.

NRSF forms complexes with multiple proteins. Through its N-terminal repressor domain, it associates with mSin3, which in turn recruits HDACs and the SWI/SNF complex [8,9,14,16,17,26]. In addition, the C-terminal repressor domain of NRSF interacts with a corepressor, CoREST, which in turn recruits a variety of corepressors/silencers, including LSD1, HDACs, MeCP2 and CtBP [14,15,18]. The NRSF zinc-finger domain mediates its DNA-binding and nuclear localization [5,6,27]. REST/NRSF-interacting LIM protein (RILP), a protein containing three LIM domains, reportedly associates with the NRSF zinc-finger domain and is involved in mediating its nuclear localization [28]. Though we did not carry out a detailed exploration of the regions involved in the binding of NRSF to RILP or Zfp90 in this study, co-expression of Zfp90 with NRSF did not disrupt their nuclear localization, suggesting that Zfp90 does not interfere with the association between RILP and NRSF.

We previously showed that class II HDACs form complexes with NRSF, and that CaMKII-mediated nuclear export of these HDACs contributes to the attenuation of NRSF repressor activity in response to hypertrophic stimuli [8]. Class II HDACs interact with mSin3 and then complex with NRSF via its N-terminal repressor domain. That expression of Zfp90 mRNA is dramatically increased in failing human hearts suggests increased cardiac expression of Zfp90 may also be involved in the attenuation of NRSF repressor function via its zinc-finger domain under pathological conditions. Thus multiple stress-responsive signaling pathways appear to modulate NRSF repressor function through different NRSF domains during the process of cardiac remodeling.

In this study, we analyzed expression of the ANP, BNP, HCN4 and SERCA2 genes in the ventricles of 12-week-old Zfp90-Tg mice. At that age there was no obvious difference in cardiac morphology or function, evaluated based on heart weight-to-body weight ratios and echocardiography, between Zfp90-Tg mice and their wild-type littermates. This eliminates the possibility that cardiac hypertrophy or dysfunction affected cardiac gene expression independently of Zfp90. That 12-week-old Zfp90-Tg mice show no significant morphological or functional abnormalities is consistent with our earlier report that transgenic mice overexpressing a dominant-negative NRSF mutant in a cardiac-specific manner show no significant cardiac morphological or functional deterioration at 12 weeks of age [20]. By contrast, alterations in the expression of NRSF-target genes apparently precede the morphological and functional changes and are detectable in mice as young as 8 weeks of age. We are currently analyzing the cardiac phenotypes of older Zfp90-Tg mice to determine whether Zfp90 overexpression is sufficient to alter normal cardiac morphology and function.

Zfp90 was originally identified through screening using oligonucleotides complementary to the conserved interfinger region of several known zinc-finger-encoding genes [25]. It is known to contain 13 zinc-finger domains and a KRAB domain and to exhibit repressor activity, but its biological function has remained only poorly understood. In the present study we report that Zfp90 is a novel NRSF binding partner that acts as a likely regulator of the cardiac fetal gene program. Through the use of an integrative genomic approach, Zfp90 was recently found to be causally involved in the susceptibility to obesity [29], acting as a central node controlling multiple obesity-related genes in a liver-specific gene network. Our findings suggest Zfp90 may also play important roles in controlling cardiac growth and remodeling by regulating a cardiac gene network. Further evaluation of the function of Zfp90 in cardiac disease would thus seem warranted.

Sources of funding

This research was supported by a Grant-in-Aid for Scientific Research from the Japan Society for the Promotion of Science (to K. Nakao and K. Kuwahara); a grant from the Japanese Ministry of Health, Labour and Welfare (to K. Nakao); grants from the Mitsubishi Foundation, the Uehara Memorial Foundation, the Japan Foundation for Applied Enzymology, the Mitsubishi Pharma Research Foundation, the Astellas Foundation for Research on Metabolic Disorders, the Vehicle Racing Commemorative Foundation, the Japan Research Promotion Society for Cardiovascular Diseases, the Takeda Medical Research Foundation and the Hoh-ansha Foundation (to K. Kuwahara).

Disclosures

None.

Acknowledgements

We thank Yukari Kubo for her excellent secretarial work and Yusuke Kobayashi for his excellent technical assistant.

Appendix A. Supplementary data

Supplementary data associated with this article can be found, in the online version, at doi:10.1016/j.yjmcc.2011.01.017.

References

[1] Olson EN. A decade of discoveries in cardiac biology. Nat Med 2004;10:467–74.
[2] Saito Y, Nakao K, Arai H, Nishimura K, Okumura K, Obata K, et al. Augmented expression of atrial natriuretic polypeptide gene in ventricle of human failing heart. J Clin Invest 1989;83:298–305.
[3] Mukoyama M, Nakao K, Hosoda K, Suga S, Saito Y, Ogawa Y, et al. Brain natriuretic peptide as a novel cardiac hormone in humans. Evidence for an exquisite dual natriuretic peptide system, atrial natriuretic peptide and brain natriuretic peptide. J Clin Invest 1991;87:1402–12.
[4] Mori N, Schoenherr C, Vandenbergh DJ, Anderson DJ. A common silencer element in the SCG10 and type II Na+ channel genes binds a factor present in nonneuronal cells but not in neuronal cells. Neuron 1992;9:45–54.
[5] Chong JA, Tapia-Ramirez J, Kim S, Toledo-Aral JJ, Zheng Y, Boutros MC, et al. REST: a mammalian silencer protein that restricts sodium channel gene expression to neurons. Cell 1995;80:949–57.
[6] Schoenherr CJ, Anderson DJ. The neuron-restrictive silencer factor (NRSF): a coordinate repressor of multiple neuron-specific genes. Science 1995;267:1360–3.
[7] Ooi L, Wood IC. Chromatin crosstalk in development and disease: lessons from REST. Nat Rev Genet 2007;8:544–54.
[8] Nakagawa Y, Kuwahara K, Harada M, Takahashi N, Yasuno S, Adachi Y, et al. Class II HDACs mediate CaMK-dependent signaling to NRSF in ventricular myocytes. J Mol Cell Cardiol 2006;41:1010–22.
[9] Naruse Y, Aoki T, Kojima T, Mori N. Neural restrictive silencer factor recruits mSin3 and histone deacetylase complex to repress neuron-specific target genes. Proc Natl Acad Sci USA 1999;96:13691–6.
[10] Ballas N, Grunseich C, Lu DD, Speh JC, Mandel G. REST and its corepressors mediate plasticity of neuronal gene chromatin throughout neurogenesis. Cell 2005;121:645–57.
[11] Andres ME, Burger C, Peral-Rubio MJ, Battaglioli E, Anderson ME, Grimes J, et al. CoREST: a functional corepressor required for regulation of neural-specific gene expression. Proc Natl Acad Sci USA 1999;96:9873–8.
[12] Grimes JA, Nielsen SJ, Battaglioli E, Miska EA, Speh JC, Berry DL, et al. The co-repressor mSin3A is a functional component of the REST–CoREST repressor complex. J Biol Chem 2000;275:9461–7.
[13] Lunyak VV, Burgess R, Prefontaine GG, Nelson C, Sze SH, Chenoweth J, et al. Corepressor-dependent silencing of chromosomal regions encoding neuronal genes. Science 2002;298:1747–52.
[14] Coulson JM. Transcriptional regulation: cancer, neurons and the REST. Curr Biol 2005;15:R665–8.
[15] Garriga-Canut M, Schoenike B, Qazi R, Bergendahl K, Daley TJ, Pfender RM, et al. 2-Deoxy-D-glucose reduces epilepsy progression by NRSF-CtBP-dependent metabolic regulation of chromatin structure. Nat Neurosci 2006;9:1382–7.
[16] Huang Y, Myers SJ, Dingledine R. Transcriptional repression by REST: recruitment of Sin3A and histone deacetylase to neuronal genes. Nat Neurosci 1999;2:867–72.
[17] Roopra A, Sharling L, Wood IC, Briggs T, Bachfischer U, Paquette AJ, et al. Transcriptional repression by neuron-restrictive silencer factor is mediated via the Sin3-histone deacetylase complex. Mol Cell Biol 2000;20:2147–57.
[18] Lee MG, Wynder C, Cooch N, Shiekhattar R. An essential role for CoREST in nucleosomal histone 3 lysine 4 demethylation. Nature 2005;437:432–5.
[19] Kuwahara K, Saito Y, Ogawa E, Takahashi N, Nakagawa Y, Naruse Y, et al. The neuron-restrictive silencer element-neuron-restrictive silencer factor system regulates basal and endothelin 1-inducible atrial natriuretic peptide gene expression in ventricular myocytes. Mol Cell Biol 2001;21:2085–97.
[20] Kuwahara K, Saito Y, Takano M, Arai Y, Yasuno S, Nakagawa Y, et al. NRSF regulates the fetal cardiac gene program and maintains normal cardiac structure and function. EMBO J 2003;22:6310–21.

[21] Ogawa E, Saito Y, Kuwahara K, Harada M, Miyamoto Y, Hamanaka I, et al. Fibronectin signaling stimulates BNP gene transcription by inhibiting neuron-restrictive silencer element-dependent repression. Cardiovasc Res 2002;53: 451–9.
[22] Kuwahara K, Teg Pipes GC, McAnally J, Richardson JA, Hill JA, Bassel-Duby R, et al. Modulation of adverse cardiac remodeling by STARS, a mediator of MEF2 signaling and SRF activity. J Clin Invest 2007;117:1324–34.
[23] Nakagawa O, Ogawa Y, Itoh H, Suga S, Komatsu Y, Kishimoto I, et al. Rapid transcriptional activation and early mRNA turnover of brain natriuretic peptide in cardiocyte hypertrophy. Evidence for brain natriuretic peptide as an "emergency" cardiac hormone against ventricular overload. J Clin Invest 1995;96:1280–7.
[24] Kawakami R, Saito Y, Kishimoto I, Harada M, Kuwahara K, Takahashi N, et al. Overexpression of brain natriuretic peptide facilitates neutrophil infiltration and cardiac matrix metalloproteinase-9 expression after acute myocardial infarction. Circulation 2004;110:3306–12.
[25] Lange R, Christoph A, Thiesen HJ, Vopper G, Johnson KR, Lemaire L, et al. Developmentally regulated mouse gene NK10 encodes a zinc finger repressor protein with differential DNA-binding domains. DNA Cell Biol 1995;14:971–81.
[26] Watanabe H, Mizutani T, Haraguchi T, Yamamichi N, Minoguchi S, Yamamichi-Nishina M, et al. SWI/SNF complex is essential for NRSF-mediated suppression of neuronal genes in human nonsmall cell lung carcinoma cell lines. Oncogene 2006;25:470–9.
[27] Shimojo M, Lee JH, Hersh LB. Role of zinc finger domains of the transcription factor neuron-restrictive silencer factor/repressor element-1 silencing transcription factor in DNA binding and nuclear localization. J Biol Chem 2001;276:13121–6.
[28] Shimojo M, Hersh LB. REST/NRSF-interacting LIM domain protein, a putative nuclear translocation receptor. Mol Cell Biol 2003;23:9025–31.
[29] Schadt EE, Lamb J, Yang X, Zhu J, Edwards S, Guhathakurta D, et al. An integrative genomics approach to infer causal associations between gene expression and disease. Nat Genet 2005;37:710–7.

Endocrinology. First published ahead of print April 26, 2011 as doi:10.1210/en.2011-0004

Impaired CNS Leptin Action Is Implicated in Depression Associated with Obesity

Nobuko Yamada, Goro Katsuura, Yukari Ochi, Ken Ebihara, Toru Kusakabe, Kiminori Hosoda, and Kazuwa Nakao

Department of Medicine and Clinical Science, Kyoto University Graduate School of Medicine, Kyoto 606-8507, Japan

Recent epidemiological studies indicate that obesity increases the incidence of depression. We examined the implication of leptin for obesity-associated depression. Leptin induced antidepressive behavior in normal mice in a forced swimming test (FST), and leptin-overexpressing transgenic mice with hyperleptinemia exhibited more antidepressive behavior in the FST than nontransgenic mice. In contrast, leptin-deficient ob/ob mice showed more severe depressive behavior in the FST than normal mice, and leptin administration substantially ameliorated this depressive behavior. Diet-induced obese (DIO) mice fed a high-fat diet showed more depressive behavior in the FST and in a sucrose preference test compared with mice fed a control diet (CD). In DIO mice, leptin induced neither antidepressive action nor increment of the number of c-Fos immunoreactive cells in the hippocampus. Diet substitution from high-fat diet to CD in DIO mice ameliorated the depressive behavior and restored leptin-induced antidepressive action. Brain-derived neurotrophic factor concentrations in the hippocampus were significantly lower in DIO mice than in CD mice. Leptin administration significantly increased hippocampal brain-derived neurotrophic factor concentrations in CD mice but not in DIO mice. The antidepressant activity of leptin in CD mice was significantly attenuated by treatment with K252a. These findings demonstrated that leptin induces an antidepressive state, and DIO mice, which exhibit severe depressive behavior, did not respond to leptin in both the FST and the biochemical changes in the hippocampus. Thus, depression associated with obesity is due, at least in part, to impaired leptin activity in the hippocampus. (*Endocrinology* 152: 0000–0000, 2011)

The obese population is progressively increasing worldwide and is rapidly becoming a major health problem. Obesity is associated with a higher risk of lifestyle-related cardiovascular and metabolic disorders, such as hypertension, diabetes, and hyperlipidemia. In addition, recent epidemiological studies demonstrated that obesity is associated with an increased risk of developing depression (1–5). The precise mechanisms underlying the interaction between obesity and depression, however, have not been elucidated.

Leptin is an adipokine secreted by adipocytes and plays a pivotal role in energy regulation, such as by decreasing food intake and increasing energy expenditure and glucose/lipid metabolism, mainly by acting in the hypothalamus of the brain (6). Moreover, leptin affects cognition and mood in the cerebral cortex and hippocampus (7). In the forced swimming test (FST) in rats, administration of leptin induces an antidepressant-like activity in the hippocampus, which is considered to be an important region for regulation of the depressive state (8), but not in the hypothalamus (9). Although obese humans and rodents usually have high circulating levels of leptin in proportion to their greater fat mass, the high concentrations of leptin neither reduce food intake nor increase energy expenditure (10). This paradoxical situation in obesity has been termed "leptin resistance" (11), which is considered to be a central dogma for obesity in humans and diet-induced obese (DIO) rodents (6).

ISSN Print 0013-7227 ISSN Online 1945-7170
Printed in U.S.A.

doi: 10.1210/en.2011-0004 Received January 4, 2011. Accepted April 7, 2011.

Abbreviations: ARC, Arcuate nucleus; BDNF, brain-derived neurotrophic factor; CA, cornu Ammonis; CD, control diet; DG, dentate gyrus; DIO, diet-induced obese; DMI, desipramine; FST, forced swimming test; HFD, high-fat diet; icv, intracerebroventricular; LepTg mice, Tg skinny mice overexpressing leptin in the liver; PFA, paraformaldehyde; RT, room temperature; Tg, transgenic; TrkB, tyrosine kinase B.

Based on these observations, we postulated that the development of depression associated with obesity might be due in part to impaired leptin activity in the hippocampus. As a first step toward gaining insight into the functional significance of leptin in regulation of the depressive state, depressive behaviors were examined in leptin-deficient ob/ob mice and transgenic (Tg) skinny mice overexpressing leptin in the liver (LepTg mice). The extent of the depressive state in DIO mice was then compared with that in normal mice, and leptin actions in DIO mice were also compared with those in normal mice. The findings from the present studies suggest that depression associated with obesity is, in part, due to impaired leptin actions activity in the hippocampus.

Materials and Methods

Animals and diets

Six-week-old male C57BL/6J mice were obtained from Japan SLC, Inc. (Shizuoka, Japan) and housed on a 12-h light, 12-h dark cycle; the lights were switched on at 0900 h and room temperature (RT) was maintained at 23 ± 1 C, and the mice had *ad libitum* access to water and food. Normal mice were randomly divided into two groups. The first group was given CE-2 as a control diet (CD) (CLEA Japan, Inc., Tokyo, Japan) containing 12.6% fat of total calories (343.1 kcal/100 g). The second group was given a high-fat diet (HFD) (no. D12492; Research Diets, Inc., New Brunswick, NJ) containing 60% fat of total calories, predominantly in the form of lard (524 kcal/100 g). Both groups were fed for 16 wk until being subjected to the experiments. In another experiment, mice maintained on a HFD for 16 wk were subjected to diet substitution from the HFD to the CD for another 3 wk, and immobility time in the FST was examined.

The generation of Tg skinny mice overexpressing leptin under the control of the human serum amyloid P component promoter on the C57BL/6J background was reported in our previous paper (12). LepTg mice and non-Tg mice were used at 9–11 wk of age in the present study. Male C57BL/6J-ob/ob mice were purchased from CLEA Japan, Inc. and used at 12–14 wk of age.

Analysis of metabolic parameters and sampling of brain regions

Blood samples were obtained from the thoracic aorta using a syringe with heparin sodium (Ajinomoto, Tokyo, Japan) and aprotinin (Bayer, Tokyo, Japan) under isoflurane (Abbott Japan, Tokyo, Japan) anesthesia between 1100 and 1500 h under free feeding conditions. After blood sampling, the mice were killed by decapitation, and the hippocampus and hypothalamus were rapidly dissected, frozen in liquid nitrogen, and stored at −80 C. The fat mass was collected and weighed. The blood samples were centrifuged 14,000 rpm for 2 min, and plasma was separated and stored at −20 C until assayed. Plasma levels of glucose, insulin, leptin, triglyceride, and corticosterone were measured in duplicate with 10-μl samples using commercially available measurement kits, glucose C2 (Wako Pure Chemical Industries, Ltd., Osaka, Japan), Glazyme insulin-EIA test (Wako Pure Chemical Industries, Ltd.), mouse leptin ELISA (Linco Research, St. Charles, MO), triglyceride E test (Wako Pure Chemical Industries, Ltd.), and correlate-EIA corticosterone enzyme immunoassay kit (Assay Designs, Inc., Ann Arbor, MI), respectively.

Changes in the plasma corticosterone levels in response to swimming were determined before pretest swimming in the FST and at 15 min, 30 min, 1 h, 2 h, and 24 h after pretest swimming in the FST, as described below.

Forced swimming test

The FST is widely accepted as a task that induces depressive behavior in depression research and has good reliability and high predictive validity for assessment of the depressive state and the detection of potential antidepressant-like activity in experimental animals (13, 14). In this test, animals display "despair" behavior as indicated by immobility and escape-oriented behaviors as indicated, in particular, by swimming (14). When a mouse is forced to swim in a glass cylinder filled with water from which they cannot escape, they eventually cease escape attempts and become immobile. In the FST, increasing immobility time indicates a more depressive state. The stress-induced behavioral despair is considered to be analogous to depression in humans (14). This test consists of a 15-min pretest swimming and a 6-min test swimming 24 h later. On the first day of the experiment, the mice were dropped individually into a glass cylinder (height, 15 cm; diameter, 12 cm) containing water (23 C) at a 10-cm depth for the 15-min pretest swimming. The stressful pretest swimming facilitates the development of immobility during the test session swimming. After the 15-min pretest swimming, each mouse was returned to its home cage. Twenty-four hours later, the duration of immobility was recorded during the last 4 min of the 6-min testing period, after a 2-min habituation period.

Sucrose preference test

The sucrose preference test is another method for evaluating the depressive state that measures an animal's responsiveness to a natural reward (15). A decreased sucrose preference is considered to be homologous to adhedonia, the inability to experience pleasure, which simulates the defining symptom of major depression (16). As described in a previous report (17), the sucrose preference test was conducted over a 72-h period using a two-bottle test, one with 3% sucrose solution and the other with water. To prevent a potential location preference for drinking, the position of the bottles was changed every 24 h. The amount of the sucrose solution or water consumed was determined by weighing the bottles. The preference for the sucrose solution was calculated as the percentage of sucrose solution ingested relative to the total amount of liquid consumed.

Effects of leptin, desipramine (DMI), brain-derived neurotrophic factor (BDNF), and K252a in the FST

To assess the antidepressant effect of leptin in CD and DIO mice, mice received three sc injections of saline, recombinant mouse leptin (0.3, 1.0, and 3.0 mg/kg; Amgen, Thousand Oaks, CA), or DMI (7.5 mg/kg; Sigma-Aldrich, Inc., St. Louis, MO), a tricyclic antidepressant used as a positive control (9), at 30 min after the 15-min pretest swimming and at 2.5 and 0.5 h before the test swimming according to an established method for pharmacological evaluation of clinically potent antidepressants, such as imipramine and DMI, in mice (9).

The coordinates for intracerebroventricular (icv) injection (2 μl/mouse) was 1.8 mm lateral from the midsagittal suture, 0.7

mm posterior to the bregma, and −2.5 mm from the flat skull surface (18). The icv injection was performed at 30 min after the 15-min pretest swimming and at 2.5 h before the test swimming according to our previous report (19). Mice received an icv injection of leptin (1 μg/2 μl per mouse), BDNF (1 μg/2 μl per mouse; Sigma-Aldrich, Inc.), or K252a (1 μg/2 μl per mouse; Tocris, Bristol, UK), an inhibitor of BDNF receptor tyrosine kinase B (TrkB) (20). Control mice received an icv injection of 2-μl saline or vehicle (10% dimethylsulfoxide in saline for K252a). At the end of the icv injection experiments, the icv injection accuracy was verified by examining the location of an injection with India ink (2 μl). Any animal with misplaced marks was excluded from the analysis.

Anorectic effect of leptin

In accordance with the method for observing the effect of leptin on FST, leptin (3.0 mg/kg) was sc injected three times as follows: 1 h before the dark phase on the first day and at 3 and 1 h before the dark phase on the second day. Nocturnal food intake was measured for 15 h after the last injection.

Immunohistochemistry for c-Fos in the brain

The method of c-Fos immunohistochemistry was based on a previous report with minor modifications (21). Mice were anesthetized with pentobarbital at 1 h after the last saline or leptin injection and perfused with 50 ml of 0.1 M PBS (Sigma-Aldrich, Inc.), followed by 50 ml ice-cold 4% paraformaldehyde (PFA) in 0.1 M PBS. The brain was removed and postfixed at 4 C with 4% PFA in 0.1 M PBS overnight, followed by 30% sucrose in 0.1 M PBS for 48 h. Sections of 30-μm thickness were cut with a cryostat. According to the mouse brain atlas (18), cross-sections of the hypothalamus and hippocampus were selected in correspondence to figure 47 (1.94 mm posterior to the bregma) and figure 51 (2.46 mm posterior to the bregma) of the mouse brain atlas. Sections were thaw-mounted onto MAS-coated slides (Matsunami, Osaka, Japan) and postfixed with 4% PFA in PBS for 15 min at RT. Antigens were unmasked by before boiling for 10 min in 0.01 M sodium citrate (pH 7.0). For permeabilization of the cell surface, sections were treated with 0.25% Triton X-100 in PBS for 10 min at RT. To enhance penetration of the antibody, sections were treated with in 0.3% H_2O_2 in PBS for 10 min at RT. To reduce nonspecific background staining, the sections were treated with 3% goat serum and 5% BSA in PBS for 30 min at RT. For c-Fos protein staining, the sections were incubated with anti-c-Fos rabbit antibody (Ab-5, 1:5000; Oncogene Science, Cambridge, MA) in PBS containing 3% goat serum, 0.3% BSA, and 0.3% Triton X-100 overnight at RT. The antibody was detected using the Vectastain ABC Elite kit (PK-6101; Vector Laboratories, Burlingame, CA). A diaminobenzidine substrate kit (SK-4100; Vector Laboratories) was used for visualization. The number of c-Fos-immunoreactive cells was counted on both sides of the arcuate nucleus (ARC) of the hypothalamus and hippocampal cornu Ammonis (CA)1–CA3 and dentate gyrus (DG).

Measurement of BDNF concentrations in the hippocampus

The method used for measuring the BDNF concentrations in the hippocampus was based on a previous report with minor modifications (22). The hippocampus was homogenized in lysis buffer (137 mM NaCl, 20 mM Tris-HCl, 1% Tergitol type Nonidet P-40, 10% glycerol, 1 mM phenylmethylsulfonyl fluoride, 10 μg/ml aprotinin, and 1 μg/ml leupeptin). After sonication, the homogenates were centrifuged at 16,000 × *g* for 30 min (4 C), and the supernatants were used for ELISA analysis. Total protein was measured by the MicroBCA method (Pierce Biotechnology, Rockford, IL). BDNF concentrations were measured using a commercially available kit (BDNF E_{max} ImmunoAssay System kit; Promega, Inc., Madison, WI) according to the manufacturer's instructions. Values were expressed as picograms BDNF per milligram protein. In the leptin treatment experiment, mice were killed at 1 h after the last injection of saline or leptin (3.0 mg/kg, sc, three times at 24, 3, and 1 h before killing), and the hippocampus was removed from each mouse. The hippocampus was quickly removed and frozen in dry ice. BDNF protein levels were assayed as described above.

Western blot analysis of TrkB

Western blotting of TrkBs in the hippocampus was performed according to a previous report (23). For detail methods, see Supplemental Methods, published on The Endocrine Society's Journals Online web site at http://endo.endojournals.org.

Ob-Rb mRNA expressions

Ob-Rb mRNA expression in the hypothalamus and hippocampus was assessed by quantitative real-time RT-PCR according to our previous report (24). Primers for Ob-Rb were as follows: sense 5′-TGTTTTGGGACGATGTTCCA-3′ and antisense 5′-CATTTGAGCATCTTTTTACCAAGC-3′ (25).

Locomotor activity

As reported in our previous paper (26), the spontaneous locomotor activity of each mouse was assessed using a Supermex (Muromachi Kikai Co., Ltd., Tokyo, Japan) for 10 min immediately after each mouse had been placed into a new cage.

Data analysis

Statistical analysis of the data were performed by ANOVA followed by the Tukey-Kramer test. Statistical significance was defined as $P < 0.05$.

Results

Effects of leptin on depressive behavior in FST

In normal mice fed CD (CD mice) in the FST, sc administration of leptin at doses of 1 and 3 mg/kg significantly decreased the immobility time compared with saline treatment with no change in body weight [saline treatment: pretreatment, 32.8 ± 0.5 g; posttreatment, 32.5 ± 0.4 g; leptin (3 mg/kg) treatment: pretreatment, 32.6 ± 0.6 g; posttreatment, 32.0 ± 0.6 g; $F(3,36) = 0.380$, $P = 0.77$] (Fig. 1A). The sc administration of DMI (7.5 mg/kg), a tricyclic antidepressant, significantly decreased the immobility time in normal mice with no change in body weight [saline treatment: pretreatment, 33.2 ± 1.3 g; posttreatment, 32.6 ± 1.4 g; DMI treatment: pretreatment, 34.6 ± 1.0 g; posttreatment, 33.7 ± 1.0 g; $F(3,18) = 0.463$, $P = 0.71$]. Moreover, icv injection of